modified assays still exists because of the small scale of their data sets. Although further data accumulation is required to clarify the reliability of the strategy, a tiered testing approach for *in vitro* photosafety assessment could be proposed on the basis of combined use of several *in vitro* photochemical and photobiochemical methodologies. The proposed assay strategy might meet the 3R requirements for "replacement" of animal testing in accordance with the 7th Amendment of the European Cosmetics Directive and would be available for non-animal experiments-based product development.

## Conflict of Interest

The authors declare that there are no conflicts of interest.

## Transparency Document

The Transparency document associated with this article can be found in the online version.

## Acknowledgments

This work was supported in part by a Health Labour Sciences Research Grant from The Ministry of Health, Labour and Welfare, Japan.

## References

Epistein, J.H., 1983. Phototoxicity and photoallergy in man. J. Am. Acad. Dermatol. 8, 141–147.

Henry, B., Foti, C., Alsante, K., 2009. Can light absorption and photostability data be used to assess the photosafety risks in patients for a new drug molecule? J. Photochem. Photobiol. B 96, 57–62.

Hino, R., Orimo, H., Kabashima, K., Atarashi, K., Nakanishi, M., Kuma, H., Tokura, Y., 2008. Evaluation of photoallergic potential of chemicals using THP-1 cells. J. Dermatol. Sci. 52, 140–143.

Hoya, M., Hirota, M., Suzuki, M., Hagino, S., Itagaki, H., Aiba, S., 2009. Development of an in vitro photosensitization assay using human monocyte-derived cells. Toxicol. In Vitro 23, 911–918.

International Conference on Harmonization of Technical Requirements for Registration of Pharmaceuticals for Human Use (ICH), 2014. ICH Guideline S10 Guidance on Photosafety Evaluation of Pharmaceuticals.

International Fragrance Association (IFRA), 2013. IFRA Standards-47th Amendment.

Liebsch, M., Spielmann, H., 2002. Currently available in vitro methods used in the regulatory toxicology. Toxicol. Lett. 127, 127–134.

Moore, D.E., 2002. Drug-induced cutaneous photosensitivity: incidence, mechanism, prevention and management. Drug Saf. 25, 345–372.

Okamoto, Y., 2005. Recent trends of alternative methods to phototoxicity testing in Japan. Altern. Anim. Test. Exp. 11, 39–48.

Okamoto, Y., Mizuno, M., Asano, H., Masunaga, T., 2002. In vitro phototoxicity of fragrance materials: evaluation in the 3T3 NRU phototoxicity test. Altern. Anim. Test. Exp. 8, 69–77.

Onoue, S., Tsuda, Y., 2006. Analytical studies on the prediction of photosensitive/phototoxic potential of pharmaceutical substanes. Pharm. Res. 23, 156–164.

Onoue, S., Kawamura, K., Igarashi, N., Zhou, Y., Fujikawa, F., Yamada, H., Tsuda, Y., Seto, Y., Yamada, S., 2008. Reactive oxygen species assay-based risk assessment of drug-induced phototoxicity: classification criteria and application to drug candidates. J. Pharm. Biomed. Anal. 47, 967–972.

Onoue, S., Seto, Y., Gandy, G., Yamada, S., 2009. Drug-induced phototoxicity; an early in vitro identification of phototoxic potential of new drug entities in drug discovery and development. Curr. Drug Saf. 4, 123–136.

Onoue, S., Suzuki, G., Kato, M., Hirota, M., Nishida, H., Kitagaki, M., Kouzuki, H., Yamada, S., 2013a. Non-animal photosafety assessment approaches for cosmetics based on the photochemical and photobiochemical properties. Toxicol. In Vitro 27, 2316–2324.

Onoue, S., Hosoi, K., Wakuri, S., Iwase, Y., Yamamoto, T., Matsuoka, N., Nakamura, K., Toda, T., Osaki, N., Matsumoto, Y., Kawakami, S., Seto, Y., Kato, M., Yamada, S., Ohno, Y., Kojima, H., 2013b. Establishment and intra-/inter-laboratory validation of a standard protocol of reactive oxygen species assay for chemical photosafety evaluation. J. Appl. Toxicol. 33, 1241–1250.

Onoue, S., Hosoi, K., Toda, T., Takagi, H., Osaki, N., Matsumoto, Y., Kawakami, S., Wakuri, S., Iwase, Y., Yamamoto, T., Nakamura, K., Ohno, Y., Kojima, H., 2014. Intra-/inter-laboratory validation study on reactive oxygen species assay for chemical photosafety evaluation using two different solar simulators. Toxicol. In Vitro 28, 515–523.

Organization for Economic Cooperation and Development (OECD), 2004. OECD Guidelines for the Testing of Chemicals Test No. 432. In Vitro 3T3 NRU Phototoxicity Test.

Scientific Committee on Consumer Safety (SCCS), 2012. The SCCS's Note of Guidance for the Testing of Cosmetic Substances and Their Safety Evaluation 8th Revision. SCCS/1501/12.

Seto, Y., Hosoi, K., Takagi, H., Nakamura, K., Kojima, H., Yamada, S., Onoue, S., 2012. Exploratory and regulatory assessments on photosafety of new drug entities. Curr. Drug Saf. 7, 140–148.

Seto, Y., Kato, M., Yamada, S., Onoue, S., 2013. Development of micellar reactive oxygen species assay for photosafety evaluation of poorly water-soluble chemicals. Toxicol. In Vitro 27, 1838–1846.

The European Agency for the Evaluation of Medicinal Products, Evaluation of Medicines for Human Use, Committee for Proprietary Medicinal Products (EMEA/CPMP), 2002. Note for Guidance on Photosafety Testing, CPMP/SWP/398/01.

The Food and Drug Administration, Center for Drug Evaluation and Research (FDA/CDER), 2002. Guidance for Industry, Photosafety Testing.

Toxicology in Vitro 33 (2016) 147–152

Contents lists available at ScienceDirect

Toxicology in Vitro

journal homepage: www.elsevier.com/locate/toxinvit

# Comparative study on prediction performance of photosafety testing tools on photoallergens

Satomi Onoue [a,*], Hiroto Ohtake [a], Gen Suzuki [a], Yoshiki Seto [a], Hayato Nishida [b], Morihiko Hirota [b], Takao Ashikaga [b], Hirokazu Kouzuki [b]

[a] Department of Pharmacokinetics and Pharmacodynamics, School of Pharmaceutical Sciences, University of Shizuoka, 52-1 Yada, Suruga-ku, Shizuoka 422-8526, Japan
[b] Shiseido Research Center, Shiseido Co. Ltd., 2-2-1 Hayabuchi, Tsuzuki-ku, Yokohama-shi, Kanagawa 226-8553, Japan

ARTICLE INFO

*Article history:*
Received 7 September 2015
Received in revised form 21 January 2016
Accepted 6 March 2016
Available online 10 March 2016

*Keywords:*
Photoallergenicity
Photosafety assessment
Phototoxicity
Reactive oxygen species
UV

ABSTRACT

Several testing methods have been established to identify potential phototoxins. The present study was undertaken to clarify the predictive ability of *in vitro* photosafety assays for photoallergenicity. On the basis of animal and/or clinical photosafety information, 23 photoallergens and 7 non-phototoxic/non-photoallergenic chemicals were selected and subjected to UV/VIS spectral analysis, reactive oxygen species (ROS)/micellar ROS (mROS) assays, and 3T3 neutral red uptake phototoxicity testing (3T3 NRU PT). Of the photoallergens tested, *ca.* 96% of chemicals had intense UV/VIS absorption with a molar extinction coefficient of over 1000 $M^{-1}$ $cm^{-1}$, and false-positive predictions were made for 3 non-photoallergenic chemicals. In the ROS assay, all photoallergens were found to be potent ROS generators under exposure to simulated sunlight. In the photosafety prediction based on the ROS assay, the individual specificity was 85.7%, and the positive predictivity and negative predictivity were found to be 95.8% and 100%, respectively. Most of the photoirritant chemicals were correctly identified by the 3T3 NRU PT; however, it provided false predictions for *ca.* 48% of photoallergens. The orders of sensitivity and specificity for photoallergenicity prediction were estimated to be: [sensitivity] ROS assay > UV/VIS absorption ≫ 3T3 NRU PT, and [specificity] 3T3 NRU PT > ROS assay ≫ UV/VIS absorption. Thus, photochemical assays, in particular the ROS assay, can be used for assessment of photoallergenicity, although there were some false-positive predictions.



## 1. Introduction

Phototoxic responses in light-exposed tissues can be caused by several classes of pharmaceuticals, cosmetics and foods, and these phototoxic events can be categorized into photoirritation, photoallergy and photogenotoxicity in accordance with their mechanisms and outcomes (Moore, 1998, 2002). Concerns about phototoxicity and its avoidance are growing, and a number of *in vitro* assay systems have been developed for photosafety assessment over the past few years (Onoue et al., 2009). The International Conference on Harmonization (ICH) S10 guidelines on photosafety evaluation successfully reached step 5 of the ICH process in 2014, describing detailed photosafety assessment strategies on the basis of photochemical and photobiochemical properties, and *in vivo* pharmacokinetic behavior (ICH, 2014). In the ICH S10 guideline, three *in vitro* photosafety test methods are recommended: (i) UV spectral analysis (Henry et al., 2009), (ii) reactive oxygen species (ROS) assay (Onoue and Tsuda, 2006), and (iii) 3T3 neutral red uptake phototoxicity test (3T3 NRU PT) (Spielmann et al., 1994).

Absorption of sunlight by phototoxins, followed by photochemical reaction, is considered to be a key trigger for phototoxicity (Onoue et al., 2013b), because photo-excited chemicals may react with biomolecules, leading to phototoxic events (Moore, 1998, 2002). In this context, the UV-absorbing property of chemicals can be a potential indicator for phototoxic risk, and Henry and co-workers demonstrated that chemicals with a molar extinction coefficient (MEC) of less than 1000 $M^{-1}$ $cm^{-1}$ showed low phototoxic risk (Henry et al., 2009). Photo-excited chemicals tend to generate ROS, resulting in oxidative damage to the cellular membrane, DNA and other biomolecules (Brendler-Schwaab et al., 2004; Epstein and Wintroub, 1985); therefore, the ROS assay of photoirradiated chemicals has been used for photosafety assessment (Onoue et al., 2014). On the other hand, 3T3 NRU PT was originally established to assess the cytotoxicity of

*Abbreviations:* 3T3 NRU PT, 3T3 neutral red uptake phototoxicity testing; AOP, Adverse Outcome Pathway; DMSO, dimethyl sulfoxide; ICH, International Conference on Harmonization of Technical Requirements for Registration of Pharmaceuticals for Human Use; IFRA, International Fragrance Association; JaCVAM, Japanese Center for the Validation of Alternative Methods; JPMA, Japan Pharmaceutical Manufacturers Association; MEC, molar extinction coefficient; mROS assay, micellar ROS assay; NaPB, sodium phosphate buffer; NBT, nitroblue tetrazolium; OECD, Organisation for Economic Co-operation and Development; PIF, photoirritation factor; ROS, reactive oxygen species; UV, ultraviolet; VIS light, visible light.

* Corresponding author.
*E-mail address:* onoue@u-shizuoka-ken.ac.jp (S. Onoue).

http://dx.doi.org/10.1016/j.tiv.2016.03.003
0887-2333/

photo-excited chemicals as an *in vitro* alternative to *in vivo* phototoxicity tests (Liebsch and Spielmann, 2002).

Photoirritation is a narrowly specified type of phototoxicity that can be defined as an inflammatory event in UV-exposed tissues, triggered by photo-oxidation of lipids and proteins in the cellular membrane (Girotti, 2001; Schothorst et al., 1972), while photoallergy is an immune response to photosensitizer-bound proteins (Tokura, 2009). The *in vitro* assays recommended in the ICH S10 guideline are well validated and have a high predictive capacity for photoirritancy of tested chemicals (ICH, 2014). Although a previous study demonstrated that the photoallergenic potential of tested chemicals might be partly identified by ROS assay (Onoue et al., 2013c), the applicability of these *in vitro* assessments for predicting photoallergenic risk is still poorly understood. Therefore, we undertook the present study to clarify the predictive performance of photochemical and photobiochemical assays for the photoallergenic potential, using a panel of 23 photoallergens and 7 non-phototoxic/non-photoallergenic chemicals (Table 1). These model chemicals were assessed by means of UV/VIS spectral analysis, ROS assay, and 3T3 NRU PT, and the results were compared.

## 2. Materials and methods

### 2.1. Chemicals

On the basis of published photosafety data and the International Fragrance Association (IFRA) standard (Bakkum and Heule, 2002; Hindsen et al., 2006; Horio et al., 1994; Kerr et al., 2010; Lovell, 1993; Lugovic et al., 2007; Moore, 2002; Murata et al., 1998; Onoue et al., 2013c; Scheinfeld et al., 2014; Tokura, 2009), 30 chemicals, including 23 photoallergens and 7 non-phototoxic chemicals, were selected for the present study (Table 1). Dimethyl sulfoxide (DMSO), erythromycin (**27**), glibenclamide (**8**), hexachlorophene (**9**), indomethacin (**11**), imidazole, ketoprofen (**13**), 8-methoxypsoralen (**2**), 4′-methylbenzylidene camphor (**24**), nitroblue tetrazolium (NBT), *p*-nitrosodimethylaniline, phenytoin (**30**), piroxicam (**18**), sulfanilamide (**20**) and tribromsalan (**22**) were bought from Wako Pure Chemical Industries (Osaka, Japan). Aspirin (**25**), bithionol (**4**), dichlorophene (**5**), enoxacin (**6**), octyl dimethyl PABA (**16**), penicillin G (**29**), pyridoxine HCl (**19**) and triclocarban (**23**) were purchased from Sigma-Aldrich Japan (Tokyo, Japan). Benzophenone (**3**), hydrochlorothiazide (**10**) and methylsalicylate (**28**) were obtained from Junsei Chemical Co. (Tokyo, Japan), and 6-methylcoumarin (**1**) was purchased from Nacalai Tesque (Kyoto, Japan). Benzocaine (**26**), fenticlor (**7**), musk ambrette (**14**) and musk xylene (**15**) were purchased from Tokyo Chemical Industry (Tokyo, Japan). Isoniazid (**12**) was obtained from LKT Laboratories (St. Paul, MN, USA). Omadine Na (**17**) was bought from Alfa Aesar (Heysham, UK). Sulfasalazine (**21**) was purchased from Fluka (St. Gallen, Switzerland). A quartz reaction container for high-throughput ROS assay (Onoue et al., 2008a) was constructed by Ozawa Science (Aichi, Japan).

### 2.2. UV/VIS spectral analysis

Each chemical was dissolved in methanol or distilled water at final concentrations of 0.001, 0.01 and 0.1 μM, and the final concentration was reduced if the tested chemical was found to be an intense UV/VIS absorber. UV/VIS absorption spectra were recorded with a UV–VIS Multipurpose Spectrophotometer MPS-2400 (Shimadzu Corporation, Kyoto, Japan) interfaced to a PC for data processing (software: UVProve Version 1.12). MEC values were determined from absorbance values for peaks tailing through 290 nm from a previous maximum absorbance, and all peaks were detected at 290 nm or higher wavelength.

**Table 1**
Test chemicals.

| No. | Chemical name | CAS number | Physical state | Color | Molecular weight | Clog $P^b$ | Category[c] |
|---|---|---|---|---|---|---|---|
| *Photoallergens* | | | | | | | |
| **1** | 6-Methylcoumarin | 92-48-8 | Powder | White | 160.05 | 1.91 | C |
| **2** | 8-Methoxypsoralen | 298-81-7 | Powder | Light yellow | 216.04 | 2.31 | C, P |
| **3** | Benzophenone | 119-61-9 | Powder | White | 182.07 | 3.18 | C |
| **4** | Bithionol | 97-18-7 | Powder | White | 353.88 | 6.16 | C |
| **5** | Dichlorophene | 97-23-4 | Powder | Light yellow | 268.01 | 4.79 | P |
| **6** | Enoxacin | 74011-58-8 | Powder | White | 320.13 | −1.60 | P |
| **7** | Fenticlor | 97-24-5 | Powder | Light yellow | 285.96 | 5.19 | C |
| **8** | Glibenclamide | 10238-21-8 | Powder | White | 493.14 | 4.24 | P |
| **9** | Hexachlorophene | 70-30-4 | Powder | White | 403.85 | 7.03 | C |
| **10** | Hydrochlorothiazide | 58-93-5 | Powder | White | 296.96 | −0.36 | P |
| **11** | Indomethacin | 53-86-1 | Powder | Yellow | 357.08 | 4.18 | P |
| **12** | Isoniazid | 54-85-3 | Powder | White | 137.06 | −0.67 | P |
| **13** | Ketoprofen | 22071-15-4 | Powder | White | 254.09 | 2.76 | P |
| **14** | Musk ambrette | 83-66-9 | Powder | Yellow | 268.11 | 3.84 | C |
| **15** | Musk xylene | 81-15-2 | Powder | White | 297.10 | 3.96 | C |
| **16** | Octyl dimethyl PABA | 21245-02-3 | Liquid | Light yellow | 277.20 | 6.16 | C |
| **17** | Omadine Na | 3811-73-2 | Powder | White | 150.00 (127.01)[a] | −0.59 | C |
| **18** | Piroxicam | 36322-90-4 | Powder | White | 331.06 | 1.89 | P |
| **19** | Pyridoxine HCl | 58-56-0 | Powder | White | 205.05 (169.07)[a] | −0.35 | P, F |
| **20** | Sulfanilamide | 63-74-1 | Powder | White | 172.03 | −0.57 | P |
| **21** | Sulfasalazine | 599-79-1 | Powder | Yellow | 398.07 | 3.99 | P |
| **22** | Tribromsalan | 87-10-5 | Powder | White | 446.81 | 6.01 | P (animal) |
| **23** | Triclocarban | 101-20-2 | Powder | White | 313.98 | 5.47 | C |
| *Non-phototoxic/non-photoallergic chemicals* | | | | | | | |
| **24** | 4′-Methylbenzylidene camphor | 36861-47-9 | Powder | White | 254.17 | 5.02 | C |
| **25** | Aspirin | 50-78-2 | Powder | White | 180.04 | 1.02 | P |
| **26** | Benzocaine | 94-09-7 | Powder | White | 165.08 | 1.92 | P |
| **27** | Erythromycin | 114-07-8 | Powder | White | 791.47 | 1.66 | P |
| **28** | Methylsalicylate | 119-36-8 | Liquid | Yellow | 152.05 | 2.33 | P |
| **29** | Penicillin G | 113-98-4 | Powder | White | 387.08 (348.11)[a] | 2.27 | P |
| **30** | Phenytoin | 57-41-0 | Powder | White | 252.09 | 2.09 | P |

[a] Number in parenthesis represents molecular weight of free compound.
[b] Calculated on ChemBioDraw Ultra 13.0 software.
[c] C, cosmetic ingredients; F, food ingredients; and P, pharmaceutics.

### 2.3. ROS assay

#### 2.3.1. Irradiation

In the ROS assays, Atlas Suntest CPS plus (Atlas Material Technology LLC, Chicago, USA) was used as reported previously (Onoue et al., 2013a, 2014). The irradiation test was carried out at 25 °C with an irradiance of *ca.* 2.0 mW/cm$^2$.

#### 2.3.2. ROS assay

The ROS assay was conducted in accordance with the validated protocol (Onoue et al., 2013a, 2014). Briefly, for the measurement of singlet oxygen, samples containing the test chemical (200 μM), *p*-nitrosodimethylaniline (50 μM) and imidazole (50 μM) in 20 mM NaPB (pH 7.4) were mixed in a tube. Two hundred microliters of the sample was transferred into a well of a plastic 96-well plate (Asahi Glass Co., Ltd., Tokyo, Japan; code number: 3881-096; clear, untreated, flat-bottomed) and checked for precipitation before light exposure. After measurement of absorbance at 440 nm using a SAFIRE microplate spectrophotometer (TECAN, Mannedorf, Switzerland), the plate was fixed in a quartz reaction container with a quartz cover, then irradiated with simulated sunlight for 1 h, and agitated on a plate shaker. Then, the UV absorbance at 440 nm was measured. For the determination of superoxide, samples containing the test chemical (200 μM) and NBT (50 μM) in 20 mM NaPB were irradiated with simulated sunlight for 1 h, and the reduction in NBT was measured in terms of the increase in absorbance at 560 nm in the same manner as for the singlet oxygen determination.

#### 2.3.3. mROS assay

The mROS assay was employed for chemicals that were untestable in the ROS assay because of limited solubility (Seto et al., 2013). Briefly, to monitor the generation of singlet oxygen, test compound (200 μM), *p*-nitrosodimethylaniline (50 μM) and imidazole (50 μM) were dissolved in 20 mM NaPB (pH 7.4) with 0.5% (v/v) Tween 20. For the determination of superoxide generation, test compound (200 μM) and NBT (50 μM) were dissolved in 20 mM NaPB (pH 7.4) with 0.5% (v/v) Tween 20. These samples were then irradiated with simulated sunlight and measured under the same conditions as for the ROS assay protocol.

### 2.4. 3T3 NRU PT

The *in vitro* 3T3 NRU PT was carried out as described in the Organisation for Economic Co-operation and Development (OECD) 432 guidelines and the European Community Official Journal (L 136/9, 08.06.2000, annexe II) with minor modification (OECD, 2004). Briefly, Balb/c 3T3 cells were maintained in culture for 24 h for monolayer formation. Two 96-well plates per test chemical were then pre-incubated with six different concentrations of the chemical in duplicate for 1 h. One plate was exposed to a dose of 5 J/cm$^2$ UVA (+Irr experiment), whereas the other plate was kept in the dark (−Irr experiment). UVA irradiation was performed using a SOL 500 Sun Simulator (Dr. Hönle AG UV Technology, München, Germany) equipped with a 500 W metal halide lamp and an H1 filter to attenuate UVB. The treatment medium was then replaced with culture medium. After 24 h, cell viability was determined by measuring neutral red uptake for 3 h; the neutral red uptake was measured at the absorbance of 540 nm using a Benchmark™ Plus microplate spectrophotometer (BioRad, Hercules, CA, USA). Cell viability at each of the six concentrations of the test chemical was compared with that of untreated controls and the percent inhibition was calculated. For prediction of the phototoxic potential, the concentration responses obtained in the presence and in the absence of UV irradiation were compared, usually at the $IC_{50}$ level, that is, the concentration that reduced cell viability to 50% of that of the untreated controls. The photoirritancy factor (PIF) was determined as follows:

$$PIF = \frac{IC_{50}(-Irr)}{IC_{50}(+Irr)}.$$

## 3. Results

### 3.1. UV/VIS spectral analysis

All the test chemicals were subjected to UV/VIS spectral analysis to evaluate photoreactivity (Table 2). Although weak UV absorption was seen for musk xylene (**15**), a weak photoallergen (SCCNFP, 2004), with an MEC value of 448 $M^{-1}$ $cm^{-1}$ (290 nm), most photoallergens exhibited potent UV/VIS absorption, with maximal MEC values of over 1000 $M^{-1}$ $cm^{-1}$. In particular, the maximal MEC values of octyl dimethyl PABA (**16**) and sulfasalazine (**21**) within the UV/VIS region were found to be 28,879 $M^{-1}$ $cm^{-1}$ (310 nm) and 33,116 $M^{-1}$ $cm^{-1}$ (366 nm), respectively. Application of the threshold MEC value (1000 $M^{-1}$ $cm^{-1}$) proposed by Henry and co-workers (Henry et al., 2009) correctly predicted *ca.* 96% of the chemicals to be photoallergenic (Table 3). Within the non-phototoxic/non-photoallergenic group, there appeared to be three false-positive predictions, since 4′-methylbenzylidene camphor (**24**), benzocaine (**26**) and methylsalicylate (**28**) exhibited intense UV absorption with MEC values of 11,876 $M^{-1}$ $cm^{-1}$ (299 nm), 17,025 $M^{-1}$ $cm^{-1}$ (290 nm), and 4722 $M^{-1}$ $cm^{-1}$ (308 nm), respectively. These observations are in agreement with previous reports that some non-phototoxic chemicals have intense UV/VIS absorption (Onoue and Tsuda, 2006), and the defined threshold (1000 $M^{-1}$ $cm^{-1}$) might not always be reliable for negative prediction of photoallergenic potential. The positive and negative predictivities of the MEC-based approach were calculated to be 88.0% and 80.0%, respectively.

### 3.2. ROS assay

The ROS assay, originally developed for photosafety assessment of drugs, can monitors the generation of ROS such as singlet oxygen and superoxide from photoirradiated chemicals (Onoue et al., 2008b; Onoue and Tsuda, 2006). A validation study of the ROS assay was carried out by the Japan Pharmaceutical Manufacturers Association (JPMA), supervised by the Japanese Center for the Validation of Alternative Methods (JaCVAM) (Onoue et al., 2013a). The ROS assay was applied to all the test chemicals (Table 2); however, 8 chemicals (*ca.* 27% of total) were found to be untestable at the final concentration of 200 μM because of poor solubility. Therefore, mROS assay employing a micellar solution was optionally applied to these chemicals (Seto et al., 2013); this complementary use of mROS assay enabled us to conduct photosafety screening on 7 of the 8 chemicals (**5**, **7**, **14**–**16**, and **23**–**24**) previously untestable at 200 μM, and on tribromsalan (**22**) at a lower concentration (100 μM). In the ROS/mROS assays (Table 2), all photoallergens exhibited significant generation of ROS on exposure to simulated sunlight. Several photoallergens, such as enoxacin (**6**) and piroxicam (**18**), could generate both singlet oxygen and superoxide; however, generation of singlet oxygen seemed to be predominant, at least in the present chemical panel. In contrast, ROS generation was negligible or weak with most non-phototoxic chemicals. In accordance with the validated criteria for ROS data {25 ($\Delta A_{440\ nm} \cdot 10^3$) for singlet oxygen and 20 ($\Delta A_{560\ nm} \cdot 10^3$) for superoxide} (Onoue et al., 2008a), 16 testable photoallergens (*ca.* 70% of total photoallergens) could be correctly identified in the ROS assay, and positive predictions could also be made for 7 untestable photoallergens upon optional application of the mROS assay. The photoallergenic potential of musk xylene (**15**) could be predicted by the ROS/mROS assay based on the significant ROS generation {singlet oxygen ($\Delta A_{440\ nm} \cdot 10^3$), 104 ± 3; and superoxide ($\Delta A_{560\ nm} \cdot 10^3$),

**Table 2**
Photosafety characterization.

| No. | Chemical name | Maximal MEC ($M^{-1}cm^{-1}$)[a] | ROS/mROS[b] Singlet oxygen ($\Delta A_{440\ nm} \cdot 103$) | ROS/mROS[b] Superoxide ($\Delta A_{560\ nm} \cdot 10^3$) | 3T3 NRU PT (PIF ) | Photosafety information: Photoirritant | Photosafety information: Photoallergenic |
|---|---|---|---|---|---|---|---|
| **Photoallergens** | | | | | | | |
| 1 | 6-Methylcoumarin | 7,502 [290 nm] | 196±11 | 112±8 | 21.3 | + | + |
| 2 | 8-Methoxypsoralen | 12,564 [299 nm] | 143±13 | 8±8 | 120.5 | + | + |
| 3 | Benzophenone | 1,305 [290 nm] | 227±21 | <1 | 10.0 | + | + |
| 4 | Bithionol | 13,253 [307nm] | 273±22 | <1 | 3.6 | + | + |
| 5 | Dichlorophene | 5,973 [290 nm] | [213±4] | [<1] | 1.9 | | + |
| 6 | Enoxacin | 12,063 [345 nm] | 516±30 | 271±24 | 119.0 | + | + |
| 7 | Fenticlor | 10,002 [303 nm] | [193±3] | [<1] | 1.4 | | + |
| 8 | Glibenclamide | 1,435 [298 nm] | 37±12 | <1 | 1.1 | | + |
| 9 | Hexachlorophene | 8,381 [298 nm] | 437±5 | <1 | 1.0 | – | + |
| 10 | Hydrochlorothiazide | 4,121 [316 nm] | 171±2 | 4±7 | 1.0 | | + |
| 11 | Indomethacin | 8,738 [290 nm] | 29±13 | 168±18 | 1.5 | + | + |
| 12 | Isoniazid | 1,251 [290 nm] | 51±12 | 95±3 | 1.0 | | + |
| 13 | Ketoprofen | 2,780 [290 nm] | 316±8 | 106±5 | 75.4 | – | + |
| 14 | Musk ambrette | 2,755 [290nm] | [224±2] | [<1] | 104.2 | – | + |
| 15 | Musk xylene | 448 [290 nm] | [104±3] | [38±7] | 29.1 | – | + |
| 16 | Octyl dimethyl PABA | 28,879 [310 nm] | [76±3] | [158±9] | 2.7 | – | + |
| 17 | Omadine Na | 6,519 [290 nm] | 239±6 | 52±6 | 2.9 | | + |
| 18 | Piroxicam | 22,389 [327 nm] | 181±29 | 204±17 | 1.0 | | + |
| 19 | Pyridoxine HCl | 7,539 [291 nm] | 421±2 | 98±2 | 3.2 | + | + |
| 20 | Sulfanilamide | 3,677 [290 nm] | 265±19 | 41±4 | 1.0 | | + |
| 21 | Sulfasalazine | 33,116 [366 nm] | 51±10 | 19±5 | 1.0 | | + |
| 22 | Tribromsalan | 21,061 [325nm] | [81±2] | [<1] | 49.0 | + | + |
| 23 | Triclocarban | 3,342 [290 nm] | [63±2] | [<1] | 1.0 | – | + |
| **Non-phototoxic/non-photoallergenicchemicals** | | | | | | | |
| 24 | 4'-Methylbenzylidene camphor | 11,876 [299 nm] | [<1] | [<1] | 1.0 | – | – |
| 25 | Aspirin | 193 [290 nm] | 3±2 | <1 | 1.0 | | |
| 26 | Benzocaine | 17,025 [290 nm] | 4±1 | 9±1 | 1.0 | – | – |
| 27 | Erythromycin | < 10 | <1 | <1 | 1.0 | – | – |
| 28 | Methylsalicylate | 4,722 [308 nm] | 25±12 | <1 | 1.0 | – | – |
| 29 | Penicillin G | 31 [318 nm] | 20±24 | 9±21 | 1.0 | – | – |
| 30 | Phenytoin | < 10 | 1±1 | <1 | 1.0 | | |

Black cells: over thresholdin MEC and ROS/mROSor phototoxicity predicted in 3T3 NRU PT; and gray cells: probable phototoxicity in 3T3 NRU PT. a) Plain numbers: MEC values at $\lambda_{max}$ observed between 290–700 nm; and italicnumbers: MEC valuesat 290 nm (shoulders). b) Plain numbers: ROS data at 200 μM; plain numbers in brackets: mROS assay at 200 M; and italic letters in brackets: mROS assay at 100 μM. Data represent mean ± SD of three repeated experiments.

38 ± 7}, in spite of the weak UV/VIS-absorbing character of this compound. Although slight generation of singlet oxygen was seen in the case of methylsalicylate (**28**), other non-phototoxic chemicals were correctly judged to be negative. The ROS and optional mROS assays did not provide any false-negative predictions in the present investigation, and photoallergenic prediction of all test chemicals could be achieved with values of individual specificity, positive predictivity and negative predictivity of 85.7%, 95.8% and 100%, respectively (Table 3). These observations suggested that the ROS/mROS assays are useful for photoallergenicity screening, although careful consideration would be required to eliminate false-positive predictions.

### 3.3. 3T3 NRU Pt

In addition to the photochemical screening systems (UV and ROS assays), the photoallergenic potential of all chemicals was also tested using the 3T3 NRU PT (Table 2), which has been employed to predict photoirritation potential on the basis of PIF values of tested chemicals. PIF can be calculated from the cell viability curve and half-maximal inhibitory concentration ($IC_{50}$) values in the presence and absence of light, and the PIF values are indicative of photosafety ["no photoirritant" (PIF < 2), "probable photoirritant" (2 ≦ PIF < 5), and "photoirritant" (PIF ≧ 5)]. Although appropriate PIF criteria for prediction of photoallergenicity have not been established, these values were tentatively employed for the present study. Among the chemicals tested, 10 photoallergenic chemicals with no photoirritant potential (**5**, **7–10**, **12**, **18**, **20–21**, and **23**), as well as all non-phototoxic/non-photoallergenic chemicals, were identified as negatives because of their low PIF values (<2). In contrast, 12 photoallergens (**1–4**, **6**, **13–17**, **19**, and **22**) were captured by the 3T3 NRU PT, and, among them, 7 chemicals (**1–4**, **6**, **19**, and **22**) were recognized as photoirritants. Since the 3T3 NRU PT was designed for the identification

**Table 3**
Predictive capacity of ROS/mROS assays and 3T3 NRU PT.

| | UV | ROS/mROS assays | 3T3 NRU PT |
|---|---|---|---|
| Sensitivity (%) | 95.7 | 100.0 | 52.2 |
| Specificity (%) | 57.1 | 85.7 | 100.0 |
| Positive predictivity (%) | 88.0 | 95.8 | 100.0 |
| Negative predictivity (%) | 80.0 | 100.0 | 38.9 |

of photoirritation, not for photoallergenicity (Onoue et al., 2009), the results of positive predictions for 7 photoirritant/photoallergenic chemicals (**1–4**, **6**, **19**, and **22**) and negative predictions for 10 photoallergens (**5**, **7–10**, **12**, **18**, **20–21**, and **23**) are not necessarily surprising. Nevertheless, the finding that 5 photoallergens (**13–17**) were positive even in the 3T3 NRU PT is interesting, suggesting that cytotoxicity via an unspecified mechanism might be involved in the pathway of photoallergenicity, or that the photoallergy-related biochemical responses could be partly detected by the 3T3 NRU PT. The sensitivity, individual specificity, positive predictivity and negative predictivity of the 3T3 NRU PT in the present study were calculated to be 52.2%, 100%, 100% and 38.9%, respectively (Table 3). These findings suggested rather limited predictive performance of the 3T3 NRU PT for photoallergenic potential.

## 4. Discussion

In the present study, three *in vitro* photosafety screening systems, UV/VIS spectral analysis, ROS assay, and 3T3 NRU PT, were applied to a panel of 30 selected chemicals to clarify their predictive performance for photoallergenic potential. These assay systems were found to be partly applicable for prediction of photoallergenicity, and their predictive capacity was ranked as follows: (i) sensitivity: ROS assay > UV/VIS absorption ≫ 3T3 NRU PT, and (ii) specificity: 3T3 NRU PT > ROS assay ≫ UV/VIS absorption. Thus, the 3T3 NRU PT seems unreliable for photoallergenicity prediction, at least with the current chemical set, whereas the *in vitro* photochemical assays could predict photoallergenicity with some false-positives.

In any type of phototoxic event, penetration and absorption of light in the skin, eyes, or other UV-exposed tissues can be a critical factor for triggering phototoxic cascades, and the absorption of photon energy by the phototoxin results in excitation of the molecule itself (Onoue et al., 2013b). Since molecular oxygen can act as the predominant acceptor of excitation energy, energy can be transferred from photo-excited chemicals to oxygen through type II photochemical reaction, resulting in the generation of singlet oxygen. Transfer of an electron or hydrogen could also lead to the formation of free radical species such as superoxide, peroxyl radicals or reactive hydroxyl radical through a type I photochemical reaction. Thus, photo-excitation of chemicals tends to produce ROS, which may be one of major causative agents of phototoxic events (Brendler-Schwaab et al., 2004; Epstein and Wintroub, 1985). On the basis of the possible mechanisms and outcomes of phototoxic events, drug-induced phototoxic skin responses can be categorized into at least three types: (i) photoirritation through oxidative damage to cellular lipids and proteins, (ii) photoallergenicity through formation of photoantigens, and (iii) photogenotoxicity through DNA damage (Epstein and Wintroub, 1985; Onoue and Tsuda, 2006).

In these pathways, the photoexcitability of applied chemicals would be a key determinant for initiation of phototoxic responses; therefore, examination of photochemical properties might be a reasonable approach for prediction of photoallergenicity. In the present study, most photoallergens were successfully identified by both UV/VIS spectral analysis and ROS assay. These assays tended to overestimate the photoallergenic potential of test chemicals, as evidenced by some false-positive predictions: 3 chemicals in the UV/VIS spectral analysis, and 1 chemical in ROS assay. Not all photo-excited chemicals will induce photochemical toxicity, because some chemicals in the excited state could release the absorbed photon energy *via* emission of fluorescence, phosphorescence or heat, and thereby return to their ground state (Seto et al., 2012). This might partly explain the limited specificity of the UV/VIS approach. In theory, the ROS assay can also provide false-positive predictions, since it may capture all photochemically active substances (Onoue and Tsuda, 2006). Some photolabile substances would be judged as positive in the ROS assay if they are potent ROS generators in their photodegradation pathways. In addition to the false-positives, a false-negative prediction was made for one photoallergen in the UV/VIS approach, although this chemical exhibited potent ROS generation in the ROS assay and photodynamic cytotoxicity in the 3T3 NRU PT. A previous study also demonstrated that some phototoxic cosmetic ingredients have subthreshold MEC values ($<1000\ M^{-1}\ cm^{-1}$), providing false-negative predictions in UV/VIS spectral analysis (Onoue et al., 2013c). The MEC criterion value was well validated, at least for photosafety screening of pharmaceutical substances (Bauer et al., 2014; Henry et al., 2009); however, a reduced threshold value might be needed to enable reliable photosafety testing of non-pharmaceutical chemicals. Further validation studies using a wide variety of model chemicals will be needed to ensure the applicability of these photochemical assay systems for photoallergenicity assessment.

3T3 NRU PT was originally developed to detect photoirritant potential, and is not designed to predict other phototoxic events, such as photoallergenicity and photogenotoxicity (Onoue et al., 2009); therefore, the limited predictive performance of 3T3 NRU PT in photoallergenicity testing is not surprising. Also, 3T3 NRU PT may make false-negative predictions for chemicals predominantly absorbing in the UVB range, since only a UVA light source is used in the assay to avoid the cytotoxic effect of UVB light on 3T3 cells (Ceridono et al., 2012). According to the Clog *P* values of tested chemicals (Table 1), some photoallergens would be poorly soluble in aqueous medium, possibly providing negative predictions in the 3T3 NRU PT. Thus, in comparison with the photochemical assays, the 3T3 NRU PT might be less effective for evaluation of photoallergenicity. The exact reason why 3T3 NRU PT can make positive predictions for at least some photoallergenic chemicals remains unclear, and further mechanistic investigations might provide a basis for modification of the assay to improve its applicability for photoallergenicity screening. It is also important to accelerate the development of new *in vitro* photosensitization assays, which should be based on the photosensitization AOP (Adverse Outcome Pathway).

In conclusion, our findings indicate that photochemical assays, in particular the ROS assay, are applicable for the prediction of photoallergenic potential. Although there were some false-positive predictions, the photochemical assays show high sensitivity for assessment of photoallergenicity. However, a better understanding of their limitations through careful validation studies would be of great value for avoiding overestimation and misleading conclusions.

## Conflict of interest

None of the authors have any conflicts of interest associated with this study.

## Transparency document

The Transparency document associated in with this article can be found, in online version.

## Acknowledgment

This work was supported in part by a Health Labour Sciences Research Grant from The Ministry of Health, Labour and Welfare, Japan (H25-iyaku-wakate-024); a grant from the Cosmetology Research

Foundation (No. 527); and a grant from the Hoyu Science Foundation (No. 31).

## References


Bakkum, R.S., Heule, F., 2002. Results of photopatch testing in Rotterdam during a 10-year period. Br. J. Dermatol. 146, 275–279.

Bauer, D., Averett, L.A., De Smedt, A., Kleinman, M.H., Muster, W., Pettersen, B.A., Robles, C., 2014. Standardized UV–vis spectra as the foundation for a threshold-based, integrated photosafety evaluation. Regul. Toxicol. Pharmacol. 68, 70–75.

Brendler-Schwaab, S., Czich, A., Epe, B., Gocke, E., Kaina, B., Muller, L., Pollet, D., Utesch, D., 2004. Photochemical genotoxicity: principles and test methods. report of a GUM task force. Mutat. Res. 566, 65–91.

Ceridono, M., Tellner, P., Bauer, D., Barroso, J., Alepee, N., Corvi, R., De Smedt, A., Fellows, M.D., Gibbs, N.K., Heisler, E., Jacobs, A., Jirova, D., Jones, D., Kandarova, H., Kasper, P., Akunda, J.K., Krul, C., Learn, D., Liebsch, M., Lynch, A.M., Muster, W., Nakamura, K., Nash, J.F., Pfannenbecker, U., Phillips, G., Robles, C., Rogiers, V., Van De Water, F., Liminga, U.W., Vohr, H.W., Wattrelos, O., Woods, J., Zuang, V., Kreysa, J., Wilcox, P., 2012. The 3T3 neutral red uptake phototoxicity test: practical experience and implications for phototoxicity testing—the report of an ECVAM-EFPIA workshop. Regul. Toxicol. Pharmacol. 63, 480–488.

Epstein, J.H., Wintroub, B.U., 1985. Photosensitivity due to drugs. Drugs 30, 42–57.

Girotti, A.W., 2001. Photosensitized oxidation of membrane lipids: reaction pathways, cytotoxic effects, and cytoprotective mechanisms. J. Photochem. Photobiol. B 63, 103–113.

Henry, B., Foti, C., Alsante, K., 2009. Can light absorption and photostability data be used to assess the photosafety risks in patients for a new drug molecule? J. Photochem. Photobiol. B 96, 57–62.

Hindsen, M., Zimerson, E., Bruze, M., 2006. Photoallergic contact dermatitis from ketoprofen in southern Sweden. Contact Dermatitis 54, 150–157.

Horio, T., Miyauchi, H., Asada, Y., Aoki, Y., Harada, M., 1994. Phototoxicity and photoallergenicity of quinolones in guinea pigs. J. Dermatol. Sci. 7, 130–135.

ICH guideline S10 Guidance on photosafety evaluation of pharmaceuticals, 2014r. International Conference on Harmonization of Technical Requirements for Registration of Pharmaceuticals for Human Use.

Kerr, A., Shareef, M., Dawe, R., Ferguson, J., 2010. Photopatch testing negative in systemic quinine phototoxicity. Photodermatol. Photoimmunol. Photomed. 26, 151–152.

Liebsch, M., Spielmann, H., 2002. Currently available in vitro methods used in the regulatory toxicology. Toxicol. Lett. 127, 127–134.

Lovell, W.W., 1993. A scheme for in vitro screening of substances for photoallergenic potential. Toxicol. in Vitro 7, 95–102.

Lugovic, L., Situm, M., Ozanic-Bulic, S., Sjerobabski-Masnec, I., 2007. Phototoxic and photoallergic skin reactions. Coll. Anthropol. 31 (Suppl. 1), 63–67.

Moore, D.E., 1998. Mechanisms of photosensitization by phototoxic drugs. Mutat. Res. 422, 165–173.

Moore, D.E., 2002. Drug-induced cutaneous photosensitivity: incidence, mechanism, prevention and management. Drug Saf. 25, 345–372.

Murata, Y., Kumano, K., Ueda, T., Araki, N., Nakamura, T., Tani, M., 1998. Photosensitive dermatitis caused by pyridoxine hydrochloride. J. Am. Acad. Dermatol. 39, 314–317.

OECD guideline for testing of chemicals, 432, 2004. *In vitro* 3T3 NRU Phototoxicity Test. The Organisation for Economic Co-operation and Development.

Onoue, S., Tsuda, Y., 2006. Analytical studies on the prediction of photosensitive/phototoxic potential of pharmaceutical substances. Pharm. Res. 23, 156–164.

Onoue, S., Igarashi, N., Yamada, S., Tsuda, Y., 2008a. High-throughput reactive oxygen species (ROS) assay: an enabling technology for screening the phototoxic potential of pharmaceutical substances. J. Pharm. Biomed. Anal. 46, 187–193.

Onoue, S., Kawamura, K., Igarashi, N., Zhou, Y., Fujikawa, M., Yamada, H., Tsuda, Y., Seto, Y., Yamada, S., 2008b. Reactive oxygen species assay-based risk assessment of drug-induced phototoxicity: classification criteria and application to drug candidates. J. Pharm. Biomed. Anal. 47, 967–972.

Onoue, S., Seto, Y., Gandy, G., Yamada, S., 2009. Drug-induced phototoxicity; an early in vitro identification of phototoxic potential of new drug entities in drug discovery and development. Curr. Drug Saf. 4, 123–136.

Onoue, S., Hosoi, K., Wakuri, S., Iwase, Y., Yamamoto, T., Matsuoka, N., Nakamura, K., Toda, T., Takagi, H., Osaki, N., Matsumoto, Y., Kawakami, S., Seto, Y., Kato, M., Yamada, S., Ohno, Y., Kojima, H., 2013a. Establishment and intra-/inter-laboratory validation of a standard protocol of reactive oxygen species assay for chemical photosafety evaluation. J. Appl. Toxicol. 33, 1241–1250.

Onoue, S., Seto, Y., Yamada, S., 2013b. High-throughput screening assays to assess chemical phototoxicity. In: Steinberg, P. (Ed.), High-throughput Screening Methods in Toxicity Testing. John Wiley&Sons, Inc., Hoboken, NJ, pp. 177–190.

Onoue, S., Suzuki, G., Kato, M., Hirota, M., Nishida, H., Kitagaki, M., Kouzuki, H., Yamada, S., 2013c. Non-animal photosafety assessment approaches for cosmetics based on the photochemical and photobiochemical properties. Toxicol. in Vitro 27, 2316–2324.

Onoue, S., Hosoi, K., Toda, T., Takagi, H., Osaki, N., Matsumoto, Y., Kawakami, S., Wakuri, S., Iwase, Y., Yamamoto, T., Nakamura, K., Ohno, Y., Kojima, H., 2014. Intra-/inter-laboratory validation study on reactive oxygen species assay for chemical photosafety evaluation using two different solar simulators. Toxicol. in Vitro 28, 515–523.

SCCNFP, 2004. Evaluation and Opinion on Musk Xylene and Musk Ketone (SCCNFP/0817/04). Scientific Committee on Cosmetic Products and Non-food products intended for Consumers.

Scheinfeld, N.S., Chernoff, K., Derek Ho, M.K., Liu, Y.C., 2014. Drug-induced photoallergic and phototoxic reactions – an update. Expert Opin. Drug Saf. 13, 321–340.

Schothorst, A.A., van Steveninck, J., Went, L.N., Suurmond, D., 1972. Photodynamic damage of the erythrocyte membrane caused by protoporphyrin in protoporphyria and in normal red blood cells. Clin. Chim. Acta 39, 161–170.

Seto, Y., Hosoi, K., Takagi, H., Nakamura, K., Kojima, H., Yamada, S., Onoue, S., 2012. Exploratory and regulatory assessments on photosafety of new drug entities. Curr. Drug Saf. 7, 140–148.

Seto, Y., Kato, M., Yamada, S., Onoue, S., 2013. Development of micellar reactive oxygen species assay for photosafety evaluation of poorly water-soluble chemicals. Toxicol. in Vitro 27, 1838–1846.

Spielmann, H., Liebsch, M., Doring, B., Moldenhauer, F., 1994. First results of an EC/COLIPA validation project of in vitro phototoxicity testing methods. ALTEX 11, 22–31.

Tokura, Y., 2009. Photoallergy. Expert. Rev. Dermatol. 4, 263–270.

Toxicology in Vitro 34 (2016) 113–119

Contents lists available at ScienceDirect

Toxicology in Vitro

journal homepage: www.elsevier.com/locate/toxinvit

# Development of fluorometric reactive oxygen species assay for photosafety evaluation

Yoshiki Seto, Hiroto Ohtake, Masashi Kato, Satomi Onoue *

*Department of Pharmacokinetics and Pharmacodynamics, School of Pharmaceutical Sciences, University of Shizuoka, 52-1 Yada, Suruga-ku, Shizuoka 422-8526, Japan*

ARTICLE INFO

*Article history:*
Received 9 February 2015
Received in revised form 22 March 2016
Accepted 28 March 2016
Available online 4 April 2016

*Keywords:*
Photosafety assessment
Fluorescent probe
1,3-diphenylisobenzofuran (DPBF)
Reactive oxygen species
Phototoxicity

ABSTRACT

The present investigation involved an attempt to develop a new reactive oxygen species (ROS) assay system for the photosafety assessment of chemicals using 1,3-diphenylisobenzofuran (DPBF), a fluorescent probe for monitoring ROS generation. The assay conditions of the fluorometric ROS (fROS) assay were optimized focusing on the solvent system, concentration of DPBF, fluorescent determination, screening run time and reproducibility. The photoreactivity of 21 phototoxic and 11 non-phototoxic compounds was assessed by fROS assay, and the obtained ROS data were compared with the results from a micellar ROS (mROS) assay and *in vitro/in vivo* phototoxicity information to confirm the predictive capacity of the fROS assay. In the optimized fROS assay, intra-day and inter-day precision levels (coefficient of variation) were found to be below 5%, and the Z'-factor for DPBF fluorescence quenching showed a large separation between positive and negative controls. Of all tested compounds, 3 false positive and 7 false negative predictions were observed in the fROS assay, and the negative predictivity for the fROS assay was found to be lower than that for the mROS assay. Although the fROS assay has some limitations, the procedures for it were highly simplified with a marked reduction in screening run time and one analytical sample for monitoring ROS generation from compounds. The fROS assay has the potential to become a new tool for photosafety assessment at an early stage of product development.



## 1. Introduction

Several chemical products, including pharmaceutics and cosmetics, can induce phototoxic reactions in the skin and eyes after exposure to sunlight, consisting of partial ultraviolet (UV) B (290–320 nm), UVA (320–400 nm) and visible light (400–700 nm) (Epstein, 1983; Moore, 2002; Onoue et al., 2009). For photosafety evaluations, a UV absorption system (Henry et al., 2009) and a 3T3 neutral red uptake phototoxicity test (Spielmann et al., 1994) were recommended in the Organisation for Economic Co-operation and Development (OECD) guidelines (OECD, 2004). In addition to these recommended methods, interest in *in vitro* photosafety evaluations on the basis of the photochemical and photobiological mechanisms, notably the generation of reactive oxygen species (ROS) from photoirradiated chemicals, has increased in the pharmaceutical and cosmetic industries. A ROS assay was developed as an *in vitro* photoreactivity assessment tool for monitoring ROS generation from photoirradiated pharmaceuticals, including singlet oxygen and superoxide (Onoue and Tsuda, 2006), and the International Council on Harmonization of Technical Requirements for Registration of Pharmaceuticals for Human Use (ICH) has recommended the ROS assay as a photosafety assessment tool in the ICH S10 guidelines for photosafety evaluation (ICH, 2013). The experimental conditions of the ROS assay were optimized (Onoue et al., 2008a; Onoue et al., 2008b) and validated (Onoue et al., 2013; Onoue et al., 2014a), offering high assay productivity and prediction capacity; however, the solubility issues of the ROS assay appeared in multi-laboratory validation studies (Onoue et al., 2013; Onoue et al., 2014a). To overcome these limitations, an albuminous ROS assay (Onoue et al., 2014b) and a micellar ROS (mROS) assay (Seto et al., 2013) were also developed for evaluation of the photoreactivity of poorly water-soluble chemicals, and it has been proposed that these ROS assay systems could have a wide range of applicability for photosafety assessment.

Although these ROS assay systems could be useful as early screening tools for photosafety assessment, challenges with the current ROS assay systems for screening purposes might still remain. In the current ROS assay systems, the preparation of two independent analytical samples is needed for monitoring the generation of both singlet oxygen and superoxide from photoirradiated chemicals, and high-energy UV irradiation is required for photosafety assessments of tested chemicals, leading to operational complexity and a long run time. To improve

*Abbreviations:* CV, coefficient of variation; DBB, *o*-dibenzoylbenzene; DMSO, dimethyl sulfoxide; DPBF, 1,3-diphenylisobenzofuran; fROS assay, fluorometric reactive oxygen species assay; $H_2O_2$, hydrogen peroxide; ICH, the International Council on Harmonization of Technical Requirements for Registration of Pharmaceuticals for Human Use; mROS assay, micellar reactive oxygen species assay; NaPB, sodium phosphate buffer; NBT, nitroblue tetrazolium; OECD, the Organisation for Economic Co-operation and Development; PABA, *p*-aminobenzoic acid; ROS, reactive oxygen species; UV, ultraviolet.

* Corresponding author.
*E-mail address:* onoue@u-shizuoka-ken.ac.jp (S. Onoue).

http://dx.doi.org/10.1016/j.tiv.2016.03.019
0887-2333/

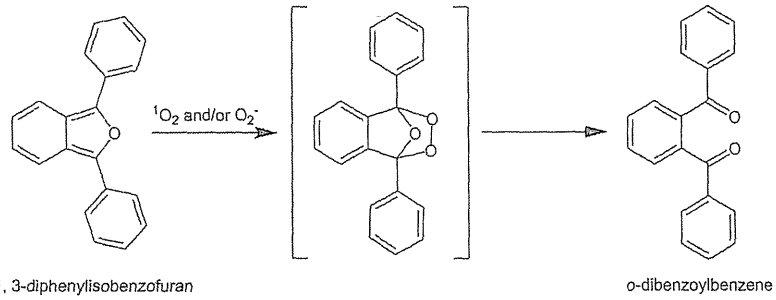


**Fig. 1.** Chemical structure and fluorescent quenching scheme of 1,3-diphenylisobenzofuran (DPBF).

these drawbacks, a novel screening strategy for monitoring ROS generation from photoirradiated chemicals would need to be developed. In the previous report, 1,3-diphenylisobenzofuran (DPBF; Fig. 1) had been used for an *in vitro* phototoxicity test on porous silicon nanoparticles (Xiao et al., 2011), and the decrease of absorbance at 410 nm caused by photobleaching of DPBF was monitored for detecting singlet oxygen generation from porous silicon nanoparticles. The operation time of the previous method was 10 min; thus the use of DPBF for detecting ROS generation may provide shorter operation time compared with the current ROS assay system. However, spectral interference between DPBF and test chemicals was concerned, possibly leading to false predictions; therefore, the colorimetrical methodology might not be appropriate for establishing a new photosafety assay. Recently, many types of fluorescent probe have been reported for detecting ROS in biological and non-biological samples (Gomes et al., 2005), and DPBF has been reported as a fluorescent probe for detecting ROS generation. DPBF in particular can detect both singlet oxygen (Wozniak et al., 1991) and superoxide (Ohyashiki et al., 1999) in phospholipid liposomes by its fluorescence decrease. DPBF changes to *o*-dibenzoylbenzene (DBB), a non-fluorescent substance, by reaction with singlet oxygen and/or superoxide. In general, fluorometric methods have higher detection sensitivity and specificity than colorimetric methods, and spectral interference can be avoided with the use of fluorometric methods. According to the previous reports, DPBF would be useful for monitoring both ROS generation from photoirradiated chemicals, and the use of a fluorescent probe might be of help to increase the productivity and usability of the ROS assay for photosafety assessments of chemicals.

The present study proposes a novel ROS assay system using DPBF, named fluorometric ROS (fROS) assay, for photosafety assessments of chemicals as an alternative to the current ROS assay systems. The assay conditions of the fROS assay were optimized, focusing on the solvent system, DPBF concentration, wavelength for the detection of DPBF fluorescence, irradiation time, sensitivity and robustness, and validation of this assay was also carried out. The fROS assay was applied to 21 phototoxic and 11 non-phototoxic compounds. To clarify the predictivity of the fROS assay, the photoreactivity of the tested chemicals was compared with the ROS data obtained from the mROS assay and *in vitro*/*in vivo* photosafety information.

## 2. Materials and methods

### 2.1. Chemicals

Chlorpromazine HCl, fenofibrate, hydrochlorothiazide, indomethacin, ketoprofen, lomefloxacin HCl, lovastatin, 6-methylcoumarin, omeprazole, pravastatin Na, cinnamic acid, erythromycin, histidine, *p*-aminobenzoic acid (PABA), penicillin G, phenytoin, dimethyl sulfoxide (DMSO), imidazole, nitroblue tetrazolium (NBT), *p*-nitrosodimethylaniline, Tween 20, disodium hydrogen phosphate 12-water and sodium dihydrogen phosphate dihydrate were obtained from Wako Pure Chemical Industries (Osaka, Japan). Cilnidipine, naproxen, benzocaine and sulisobenzone were purchased from Tokyo Chemical Industry (Tokyo, Japan). Diclofenac Na, doxycycline HCl, fluphenazine 2HCl, nalidixic acid, quinine HCl, sparfloxacin, aspirin, bumetrizole and chlorhexidine were purchased from Sigma-Aldrich Japan (Tokyo, Japan). Amlodipine, atorvastatin and enoxacin were purchased from LKT Laboratories (St. Paul, MN, USA). DPBF was obtained from Kanto Chemical (Tokyo, Japan).

### 2.2. Irradiation conditions

Chemicals were stored in an Atlas Suntest CPS + solar simulator (Atlas Material Technology LLC, Chicago, IL, USA) equipped with a xenon arc lamp (1500 W) and cooling unit SR-P20FLE (Hitachi, Tokyo, Japan). A UV special filter (# 56052371, Atlas) was installed to adapt the spectrum of the artificial light source to natural daylight, and the Atlas Suntest CPS series has high irradiance capability that meets CIE85/1989 daylight simulation requirements. The irradiation test was carried out at 25 °C with irradiance of *ca.* 2.0 mW/cm$^2$ as determined using the calibrated UVA detector Dr. Hönle # 0037 (Dr. Hönle, Munich, Germany).

### 2.3. Fluorescence spectrum analysis

DPBF (10 μM) was dissolved in 20 mM sodium phosphate buffer (NaPB; pH 7.4) containing 0.5% (*v*/*v*) Tween 20 with or without 1.5% (*w*/*v*) hydrogen peroxide ($H_2O_2$), and the mixture was incubated at room temperature for 15, 30, 45, 60, and 90 min. These procedures were carried out in the dark. After incubation, fluorescence spectra of DPBF (excitation: 414 nm) were collected using SAFIRE (TECAN, Männedorf, Switzerland).

### 2.4. Fluorometric reactive oxygen species (fROS) assay

ROS generation from irradiated compounds was qualitatively monitored by conversion from DPBF to DBB. Each tested compound was dissolved in DMSO at 10 mM as a stock solution. Samples containing compounds (200 μM) and DPBF (10 μM) in 20 mM NaPB (pH 7.4) with 0.5% (*v*/*v*) Tween 20 were prepared in the dark. As a vehicle, a sample containing DPBF (10 μM) in 20 mM NaPB (pH 7.4) with 0.5% (*v*/*v*) Tween 20 was also prepared in the dark. The samples were irradiated with simulated sunlight for 1.5 min. Fluorescence from DPBF (excitation: 414 nm and emission: 487 nm) was measured using SAFIRE before and after irradiation. To monitor ROS generation from irradiated chemicals, the obtained data were analyzed using the following equations: (i) [Fluorescence data (% of initial)] = A/B × 100. A and B represent fluorescence values for samples before and after irradiation, respectively; (ii) [Fluorescence quenching (% of vehicle)] = (C–D)/C × 100. C and D represent fluorescence data (% of initial) for vehicle and tested chemical groups, respectively.

### 2.5. Micellar reactive oxygen species (mROS) assay

For the qualitative detection of both singlet oxygen and superoxide generation from irradiated compounds, mROS assay was carried out as we reported previously (Seto et al., 2013). Briefly, each tested compound was dissolved in DMSO at 10 mM as a stock solution. For the determination of singlet oxygen generation, compounds (200 μM), *p*-nitrosodimethylaniline (50 μM) and imidazole (50 μM) were dissolved in 20 mM NaPB (pH 7.4) with 0.5% (*v*/*v*) Tween 20. To monitor the generation of superoxide, compounds (200 μM) and NBT (50 μM) were dissolved in 20 mM NaPB (pH 7.4) with 0.5% (*v*/*v*) Tween 20. These samples were irradiated with simulated sunlight for 60 min, and the decrease in absorbance at 440 nm and the increase in the absorbance at 560 nm were measured using SAFIRE for the determination of singlet oxygen and superoxide generation, respectively.

### 2.6. Z'-factor

To evaluate the robustness of the fROS assay, Z'-factor, a statistical function was estimated using the following equation: $Z' = 1 - (3\sigma_{c+} + 3\sigma_{c-})/|\mu_{c+} - \mu_{c-}|$ (Zhang et al., 1999). The means of positive and negative control signals are denoted as $\mu_{c+}$ and $\mu_{c-}$, respectively. The standard deviations of positive and negative control signals are denoted as $\sigma_{c+}$ and $\sigma_{c-}$, respectively. The difference between the means, $|\mu_{c+} - \mu_{c-}|$, defined the assay's dynamic range.

### 2.7. Criteria for data acceptance and judgment in the mROS assay

According to the results (mean of triplicate determinations) from the mROS assay, photoreactivity for each tested chemical should be judged to be (i) positive with singlet oxygen ($\Delta A_{440\ nm} \times 10^3$): 25 or more, and/or superoxide ($\Delta A_{560\ nm} \times 10^3$): 20 or more; or (ii) negative with singlet oxygen ($\Delta A_{440\ nm} \times 10^3$): less than 25, and superoxide ($\Delta A_{560\ nm} \times 10^3$): less than 20. In the mROS assay, the final decision should be made as follows: (i) positive: above the threshold level for singlet oxygen or superoxide; or (ii) negative: below the threshold level for both singlet oxygen and superoxide.

## 3. Results and discussion

### 3.1. Development of fROS assay

To develop the fROS assay, 20 mM NaPB (pH 7.4), the solvent system of the ROS assay, was applied for dissolving DPBF (10 μM); however, fluorescence emitted from DPBF could not be detected due to formation of its non-fluorescent dimer in water (Merkel and Kearns, 1972). On the other hand, DPBF-incorporated phospholipid liposomes exhibited fluorescence emission in an aqueous condition, and DPBF could detect singlet oxygen (Wozniak et al., 1991) and superoxide (Ohyashiki et al., 1999) by DPBF fluorescence quenching. Previously, the mROS assay using the micellar solution of 0.5% (*v*/*v*) Tween 20 was proposed for the photosafety assessments of poorly water-soluble chemicals (Seto et al., 2013); therefore, 20 mM NaPB (pH 7.4) containing 0.5% (*v*/*v*) Tween 20 was employed for the solvent system of the fROS assay, and up to 20 μM DPBF could be dissolved in the solvent system. On the basis of the results from the preliminary experiments, the concentration of DPBF in the solvent system and excitation wavelength of DPBF fluorescence was set at 10 μM and 414 nm, respectively, for the following experiments (data not shown). To confirm fluorescence quenching of DPBF by ROS in 20 mM NaPB (pH 7.4) containing 0.5% (*v*/*v*) Tween 20 and to determine the emission wavelength of DPBF fluorescence, fluorescent spectrum analysis on DPBF treated with 1.5% (*w*/*v*) $H_2O_2$ was conducted (Fig. 2A). Low and high peaks of the DPBF fluorescence spectrum were observed at approximately 450 and 487 nm, respectively, and the fluorescence was quenched with 1.5% (*w*/*v*) $H_2O_2$ in a time-dependent manner. Referring to the results from the fluorescent

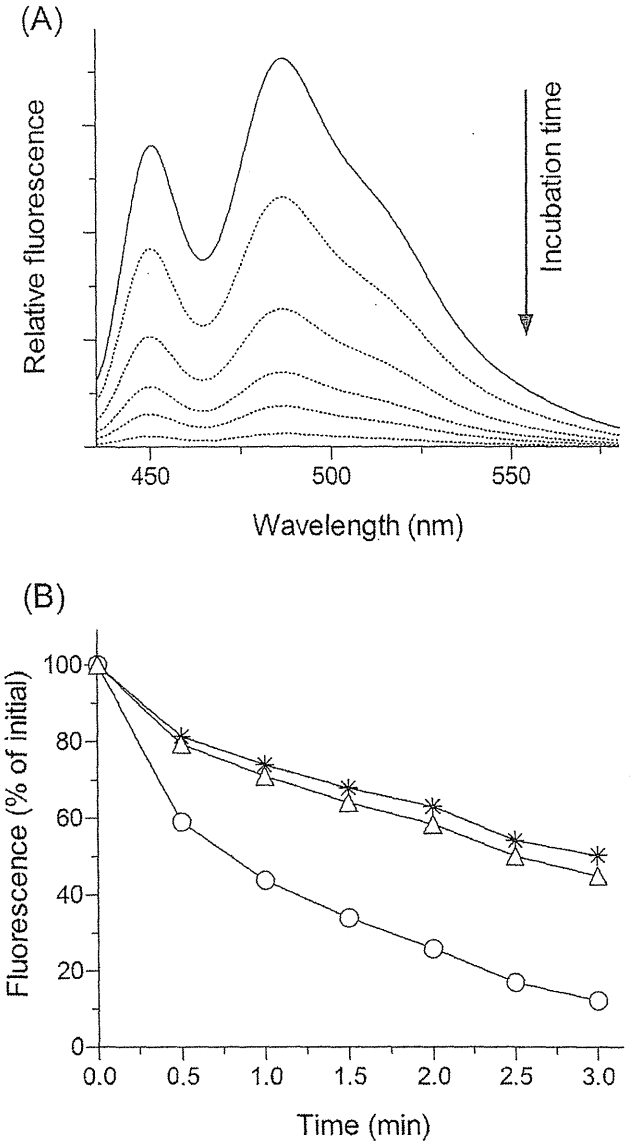


**Fig. 2.** Fluorescence quenching experiments on DPBF in 20 mM NaPB (pH 7.4) containing 0.5% (*v*/*v*) Tween 20. (A) Fluorescence spectra of DPBF. DPBF (10 μM) was incubated with or without 1.5% (*w*/*v*) $H_2O_2$ at room temperature for the indicated time (15, 30, 45, 60, and 90 min). Solid line, without 1.5% (*w*/*v*) $H_2O_2$; and dotted lines, with 1.5% (*w*/*v*) $H_2O_2$. (B) Time course of DPBF fluorescence quenching. DPBF (10 μM) was exposed to simulated sunlight with control chemicals (200 μM) for the indicated periods with irradiance of 2.0 mW/cm². △, control (vehicle alone); ○, quinine HCl (positive control); and *, sulisobenzone (negative control).

spectrum analysis, the quenching capacity at 487 nm was higher than that at 450 nm, and the emission wavelength of DPBF fluorescence for the fROS assay was determined at 487 nm.

In the current ROS assay systems, the probes for monitoring ROS generation from photoirradiated chemicals were also exposed to simulated sunlight (Onoue et al., 2008a). Although DPBF was found to be able to capture ROS under the selected solvent system, its tolerance to photoirradiation was still unclear. Thus, to optimize the irradiation time of the fROS assay, DPBF fluorescence intensity was monitored within 3 min after exposure to simulated sunlight with or without control chemicals (Fig. 2B). In the present investigation, quinine HCl and sulisobenzone were employed as positive and negative controls, respectively, the photoreactivity data of which were previously reported (Onoue et al., 2013). The fluorescence intensity of DPBF in all groups

was decreased in an irradiation time-dependent manner and, in particular, quinine HCl (200 μM) exhibited potent fluorescence quenching of DPBF at 0.5 min or later after irradiation, suggesting that the reaction of DPBF to ROS yielded from irradiated quinine HCl. Although the irradiation time of the current ROS assay system was 60 min with the same solar simulator, the fROS assay employing DPBF could be completed within a few minutes, contributing to improved throughput of photosafety screening. On the other hand, potent fluorescence quenching of DPBF by long exposure to simulated sunlight was also suspected as the fluorescence intensity of DPBF was shown to be less than 60% of the initial level at 2 min or later after irradiation of simulated sunlight. According to the data obtained from the time course of DPBF fluorescence, exposure of chemicals to simulated sunlight for 1.5 min was employed as irradiation time for the fROS assay, and the differences of fluorescence intensity between vehicle and tested chemicals were employed for evaluating the photoreactivity of tested chemicals.

### 3.2. Validation of fROS assay for photosafety assessment

To assess the robustness and reproducibility of the fROS assay, the Z'-factor was estimated (Zhang et al., 1999). The Z'-factor was designed to reflect both assay signal-to-noise ratio and the variation associated with the signal measurements. Hence, the Z'-factor is commonly utilized for quality assessment in assay development and optimization, as well as evaluation of the reproducibility of assays for high-throughput screening. In an ideal assay, the Z'-factor is close to 1.0. In practical terms, a Z'-factor greater than 0.5 is indicative of an excellent assay, whereas assays with Z'-factor values of less than 0.5 show a small separation band. The ROS generation from photoirradiated quinine HCl (200 μM) and sulisobenzone (200 μM) under 1.5-min exposure to simulated sunlight was measured 21 times (Fig. 3). The Z'-factor for the fROS assay was estimated to be 0.73, demonstrating that the fROS assay had a large separation band between positive and negative controls.

The overall precision of the method was evaluated by analyzing the fluorescence quenching of DPBF by quinine HCl and sulisobenzone at 200 μM under 1.5-min exposure to simulated sunlight. The intra-day precision ($n = 9$) and inter-day precision (days 1 to 3, $n = 9$) are shown in Table 1. The intra-day coefficient of variation (CV) for ROS generation from irradiated quinine HCl was found to be 1.5%, and the CV value of the inter-day was calculated to be 3.9%. On the basis of the data obtained, the fROS assay would have potent intra-day and inter-day precision for monitoring ROS generation from photoreactive substances. From these findings, the fROS assay would be suitable for evaluating the photoreactivity of chemicals with high throughput.

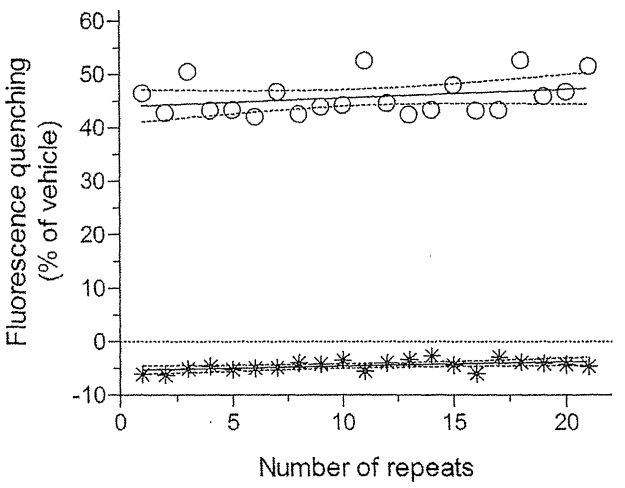


**Fig. 3.** Representative multiple measurement data used to calculate the Z'-factor for the fROS assay. ○, quinine HCl (positive control) at 200 μM; and *, sulisobenzone (negative control) at 200 μM. Solid and dashed lines represent mean and 95% confidence interval, respectively.

**Table 1**
Intra-day and inter-day precision of fROS assay.

| Compounds (200 μM) | Fluorescence quenching (% of vehicle) | |
|---|---|---|
| Intra-day (n = 9) | | |
| Quinine HCl | 43.2 ± 0.7 | [1.5] |
| Sulisobenzone | −4.5 ± 0.7 | |
| Inter-day (n = 9) | | |
| Quinine HCl | 45.2 ± 1.7 | [3.9] |
| Sulisobenzone | −4.8 ± 1.0 | |

Compounds were dissolved in 20 mM NaPB (pH 7.4) containing 0.5% (v/v) Tween 20 and exposed to simulated sunlight (2.0 mW/cm$^2$) for 1.5 min. Data represent mean ± SD of nine experiments for intra-day and intra-day precision. Values in parentheses are CV (%).

### 3.3. Photoreactivity assessment of chemicals using fROS assay

Under the optimized conditions, the fROS assay was carried out for evaluation of the photoreactivity of 21 phototoxic and 11 non-phototoxic compounds (Table 2). For comparison, the mROS assay was also conducted on these tested chemicals because the same solvent system is employed in fROS and mROS assays. Of all phototoxic compounds tested, the results for 14 phototoxic compounds, namely chlorpromazine HCl, cilnidipine, diclofenac Na, enoxacin, fenofibrate, fluphenazine 2HCl, hydrochlorothiazide, ketoprofen, lomefloxacin HCl, 6-methylcoumarin, nalidixic acid, naproxen and omeprazole, were indicative of potent DPBF fluorescence quenching upon exposure to simulated sunlight. The values of fluorescence quenching of DPBF for these compounds were calculated to be over 10% of the vehicle, and the obtained data for these compounds were consistent with those from the mROS assay. In contrast, 7 phototoxic compounds out of 21 phototoxic compounds did not exhibit DPBF fluorescence quenching upon simulated sunlight exposure, whereas ROS generation from these compounds except for indomethacin could be detected by mROS assay. Among 11 non-phototoxic compounds, 7 non-phototoxic compounds exhibited no fluorescence quenching of DPBF, while 4 non-phototoxic compounds did such quenching. The ROS data on non-phototoxic chemicals obtained from the fROS assay were inconsistent with those from the mROS assay.

### 3.4. Predictive capacity and assay limitations

To confirm the data distribution of the fROS assay, the values of DPBF fluorescence quenching were plotted, as shown in Fig. 4A. According to the results from the tested phototoxic compounds, a tentative threshold of DPBF fluorescence quenching was set at 10% of the vehicle for judging the photoreactivity of chemicals by fROS assay, and chemicals over this threshold were judged as photoreactive compounds. Then, positive and negative predictivity levels of fROS and mROS assays were compared with the *in vitro/in vivo* phototoxicity (Fig. 4B). On the basis of the photosafety information on 21 phototoxic and 11 non-phototoxic compounds, 14 phototoxic and 8 non-phototoxic compounds were correctly categorized as photoreactive and less photoreactive, respectively, using the tentative threshold of the fROS assay. In contrast, 3 false positives, namely, benzocaine, bumetrizole and PABA, and 7 false negatives, namely, amlodipine, atorvastatin, doxycycline HCl, indomethacin, lovastatin, pravastatin Na and sparfloxacin, were also identified in the fROS assay. In the mROS assay, 20 phototoxic and 7 non-phototoxic compounds were consistent with their photosafety information, and 5 chemicals, namely, indomethacin, cinnamic acid, L-histidine, penicillin G and phenytoin, were found to be false predictions. Individual specificities for the fROS and mROS assays were same, and the value was estimated to be 72.7%. The positive and negative predictivities were found to be 82.6% and 53.3% for the fROS assay and 87.0% and 88.9% for the

**Table 2**
fROS and mROS data for tested chemicals.

| No. | Compounds (200 μM) | CAS No. | fROS assay | mROS assay | | Sources of photosafety information |
|---|---|---|---|---|---|---|
| | | | Fluorescence quenching (% of vehicle) | $^1O_2$ ($\Delta A_{440\ nm} \cdot 10^3$)[a] | $O_2^-$ ($\Delta A_{560\ nm} \cdot 10^3$)[b] | |
| Phototoxic chemicals | | | | | | |
| 1 | Amlodipine | 88150-42-9 | <0 | 4±2 | 631±18 | Grabczynska and Cowley (2000) |
| 2 | Atorvastatin | 134523-00-5 | <0 | 846±9 | 844±5 | Package insert |
| 3 | Chlorpromazine HCl | 69-09-0 | 84.5±1.1 | 8±3 | 60±8 | Spielmann et al. (1998) |
| 4 | Cilnidipine | 132203-70-4 | 23.9±1.4 | 2±1 | 891±8 | Package insert |
| 5 | Diclofenac Na | 15307-79-6 | 15.6±1.2 | 451±5 | N.D. | Moore (2002) |
| 6 | Doxycycline HCl | 10592-13-9 | <0 | 114±9 | 575±2 | Moore (2002); Spielmann et al. (1994) |
| 7 | Enoxacin | 74011-58-8 | 13.5±0.7 | 454±19 | 852±8 | Lipsky and Baker (1999); Moore (2002) |
| 8 | Fenofibrate | 49562-28-9 | 99.9±0.0 | 488±6 | 208±4 | Peters and Holzhutter (2002); Spielmann et al. (1998) |
| 9 | Fluphenazine 2HCl | 146-56-5 | 82.4±0.4 | 406±11 | 377±3 | Miolo et al. (2006) |
| 10 | Hydrochlorothiazide | 58-93-5 | 24.2±2.4 | 310±6 | N.D. | Moore (2002) |
| 11 | Indomethacin | 53-86-1 | <0 | 23±2 | N.D. | Moore (2002) |
| 12 | Ketoprofen | 22071-15-4 | 99.3±0.3 | 568±4 | 619±10 | Moore (2002); Spielmann et al. (1998) |
| 13 | Lomefloxacin HCl | 98079-52-8 | 12.6±0.9 | 593±7 | 786±8 | Hayashi et al. (2004); Moore (2002) |
| 14 | Lovastatin | 75330-75-5 | <0 | 63±1 | 7±1 | Quiec et al. (1995) |
| 15 | 6-Methylcoumarine | 92-48-8 | 11.0±0.6 | 76±3 | 67±14 | Peters and Holzhutter (2002); Spielmann et al. (1998) |
| 16 | Nalidixic acid | 389-08-2 | 47.8±0.8 | 246±14 | 634±10 | Moore (2002); Peters and Holzhutter (2002) |
| 17 | Naproxen | 22204-53-1 | 39.5±4.4 | 207±7 | 257±9 | Moore (2002) |
| 18 | Omeprazole | 73590-58-6 | 16.4±0.8 | 297±6 | 51±2 | Gebhardt et al. (2012) |
| 19 | Pravastatin Na | 81131-70-6 | <0 | 9±2 | 62±7 | Package insert |
| 20 | Quinine HCl | 6119-47-7 | 45.4±1.0 | 446±21 | 862±6 | Moore (2002) |
| 21 | Sparfloxacin | 110871-86-8 | <0 | 21±8 | 42±3 | Hayashi et al. (2004); Lipsky and Baker (1999) |
| Non-phototoxic chemicals | | | | | | |
| 22 | Aspirin | 50-78-2 | <0 | 1±1 | N.D. | Onoue and Tsuda (2006) |
| 23 | Benzocaine | 94-09-7 | 13.3±1.7 | 4±1 | N.D. | Onoue and Tsuda (2006) |
| 24 | Bumetrizole | 3896-11-5 | 45.5±1.3 | N.D. | N.D. | Onoue et al. (2013) |
| 25 | Chlorhexidine | 55-56-1 | <0 | 20±4 | N.D. | Peters and Holzhutter (2002); Spielmann et al. (1994) |
| 26 | Cinnamic acid | 140-10-3 | <0 | 6±2 | 69±2 | Spielmann et al. (1995) |
| 27 | Erythromycin | 114-07-8 | <0 | 4±1 | 12±1 | Onoue and Tsuda (2006) |
| 28 | L-Histidine | 71-00-1 | 2.5±0.6 | 8±3 | 35±3 | Spielmann et al. (1994); Spielmann et al. (1995) |
| 29 | PABA | 151-13-0 | 33.4±2.0 | 8±2 | N.D. | Peters and Holzhutter (2002); Spielmann et al. (1995) |
| 30 | Penicillin G | 113-98-4 | <0 | 10±2 | 40±4 | Spielmann et al. (1994); Spielmann et al. (1995) |
| 31 | Phenytoin | 57-41-0 | <0 | 13±1 | 20±1 | Onoue and Tsuda (2006) |
| 32 | Sulisobenzone | 4065-45-6 | <0 | N.D. | 10±1 | Onoue and Tsuda (2006) |

The fROS assay and the mROS assay were carried out for tested compounds (200 μM). Data represent mean ± SD of three experiments. N.D.: not detected.
[a] Decrease in $A_{440\ nm} \times 10^3$.
[b] Increase in $A_{560\ nm} \times 10^3$.

mROS assay, respectively. According to the prediction capacities, the fROS assay was indicative of lower negative prediction than the mROS assay and thus the prediction accuracy of the fROS assay was limited under the present conditions.

To clarify the relevance of the results between the fROS and mROS assays, a 3D plot of the data obtained from both assays was produced, as shown in Fig. 4C. On the basis of this 3D plot, most of the phototoxic chemicals, from which marked ROS generation was detected by mROS assay, could be correctly judged by fROS assay; however, ROS generation from 3 phototoxic chemicals, including amlodipine, atorvastatin and doxycycline HCl, was negligible in the fROS assay, even if their photoreactivity was significant in the mROS assay. Four other false negative predictions in the fROS assay, namely, indomethacin, lovastatin, pravastatin Na and sparfloxacin, exhibited comparatively low ROS generation in the mROS assay among the tested phototoxic chemicals. In the fROS assay, photon energy required for detecting ROS generation from irradiated chemicals would be low because of the high detection sensitivity of DPBF. However, ROS generation from false negatives might be too low to be detected by DPBF under the present conditions, and thus, the DPBF fluorescence quenching by false negatives could not be observed in the fROS assay. Notably, indomethacin, identified as a false negative in both assays, was correctly categorized as a photoreactive chemical in the ROS assay (Seto et al., 2013), and thus Tween 20 might disturb the ROS generation from irradiated indomethacin. In addition to the false negatives, false positive predictions were observed in the fROS assay, such as for benzocaine, bumetrizole and PABA, even though ROS generation from them was extremely low or negligible in the mROS assay. The false positive predictions in the fROS assay might have been caused by various interactions between tested chemicals and DPBF without ROS generation. Notably, bumetrizole indicated strong DPBF fluorescence quenching, the value of which was over 50% of the vehicle, before irradiation with simulated sunlight. Thus, bumetrizole was wrongly judged as positive by fROS assay although the ROS generation from irradiated bumetrizole was negligible in the ROS assay (Onoue et al., 2013). It is suggested that the photoreactivity of chemicals reacting with DPBF before irradiation could not be evaluated by fROS assay. Although some false predictions were observed, the fROS assay using DPBF has some advantages as a screening system for evaluating photosafety of chemicals. The simplified procedures and short operation time of the fROS assay were attractive for evaluating the photoreactivity of chemicals. Compared with the current ROS assay, the fROS assay would have improved applicability to chemicals because the micellar solution of 0.5% (v/v) Tween 20 offers the solubilization of poorly water-soluble chemicals (Onoue et al., 2008c). On the other hand, in our previous study, 2 chemicals out of 83 tested chemicals could not be dissolved at the final concentration of 200 μM in the micellar solution (Seto et al., 2013). Thus, the solubilizing potency of micellar system might not be always enough for chemicals with high lipophilicity. In the ROS assay systems, the small volumes of solutions containing each reagent or test chemical are mixed in the chambers of a multi-well microplate, and then the microplates are stored in a solar simulator. The ROS data on multiple chemicals can be obtained at the same time; therefore, the fROS assay may be a productive assessment system for photosafety. According to the present outcomes, the ROS

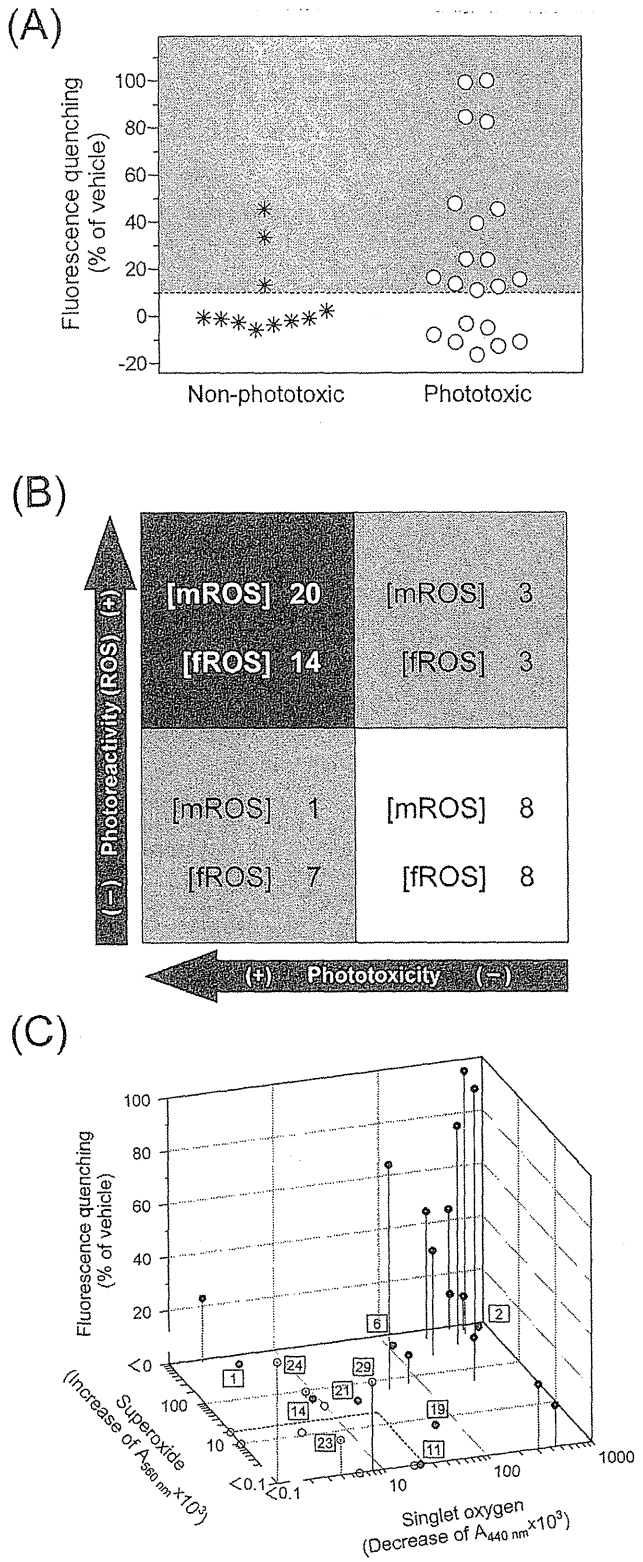


**Fig. 4.** Predictive capacity of the fROS assay. (A) Plots of fROS data for 32 tested chemicals. The chemicals in gray region would be photoreactive. (B) Positive and negative predictivity of the mROS and fROS assays as compared with the *in vitro/in vivo* phototoxicity. (C) 3D plot of mROS data (singlet oxygen generation and superoxide generation) *versus* fROS data (DPBF fluorescence quenching). Dotted lines indicate criteria of the mROS assay. The numbers located near symbols represent the chemical number of false predictions in the fROS assay. ●, phototoxic compounds; and ○, non-phototoxic compounds.

assay using fluorescent probes should be useful for the photosafety evaluation of chemicals at an early stage of product development.

## 4. Conclusion

The present investigation proposed a novel ROS assay system using fluorescence probes for evaluating the photosafety of newly developed chemicals. The photoreactivity of 32 model compounds was assessed by fROS and mROS assays, and the individual specificities for the fROS and mROS assays were same; however, the negative predictivity for the fROS assay was lower than that for the mROS assay. Although some false predictions were observed, the fROS assay using DPBF exhibited simplified assay procedures with 40-fold reduction of screening run time and a single analytical sample for monitoring ROS generation from irradiated chemicals in comparison with the ROS and mROS assays. The outcomes suggest the utility of fluorescent probes for the photosafety assessment of candidates at an early stage of product development.

## Conflict of interest

None of the authors have any conflicts of interest associated with this study.

## Transparency document

The Transparency document associated with this article can be found, in online version.

## Acknowledgement

This work was supported in part by a Health Labour Sciences Research Grant from The Ministry of Health, Labour and Welfare, Japan [H25-iyaku-wakate-024]; a grant from the Takeda Science Foundation; a grant from the Cosmetology Research Foundation [No. 527]; and a grant from the Hoyu Science Foundation [No. 31].

## References

Epstein, J.H., 1983. Phototoxicity and photoallergy in man. J. Am. Acad. Dermatol. 8, 141–147.
Gebhardt, E., Eberlein, B., Przybilla, B., Gilbertz, K.P., Placzek, M., 2012. In vitro evaluation of phototoxic properties of proton pump inhibitors, H2-receptor antagonists and statins. Acta Derm. Venereol. 92, 208–210.
Gomes, A., Fernandes, E., Lima, J.L., 2005. Fluorescence probes used for detection of reactive oxygen species. J. Biochem. Biophys. Methods 65, 45–80.
Grabczynska, S.A., Cowley, N., 2000. Amlodipine induced-photosensitivity presenting as telangiectasia. Br. J. Dermatol. 142, 1255–1256.
Hayashi, N., Nakata, Y., Yazaki, A., 2004. New findings on the structure-phototoxicity relationship and photostability of fluoroquinolones with various substituents at position 1. Antimicrob. Agents Chemother. 48, 799–803.
Henry, B., Foti, C., Alsante, K., 2009. Can light absorption and photostability data be used to assess the photosafety risks in patients for a new drug molecule? J. Photochem. Photobiol. B 96, 57–62.
International Council on Harmonisation of Technical Requirements for Registration of Pharmaceuticals for Human Use (ICH), 2013. ICH Guideline S10 Guidance on Photosafety Evaluation of Pharmaceuticals.
Lipsky, B.A., Baker, C.A., 1999. Fluoroquinolone toxicity profiles: a review focusing on newer agents. Clin. Infect. Dis. 28, 352–364.
Merkel, P.B., Kearns, D.R., 1972. Radiationless decay of singlet molecular oxygen in solution. An experimental and thepretical study of electronic-to-vibrational energy transfer. J. Am. Chem. Soc. 94, 7244–7253.
Miolo, G., Levorato, L., Gallocchio, F., Caffieri, S., Bastianon, C., Zanoni, R., Reddi, E., 2006. In vitro phototoxicity of phenothiazines: involvement of stable UVA photolysis products formed in aqueous medium. Chem. Res. Toxicol. 19, 156–163.
Moore, D.E., 2002. Drug-induced cutaneous photosensitivity: incidence, mechanism, prevention and management. Drug Saf. 25, 345–372.
The Organisation for Economic Co-operation and Development (OECD), 2004. OECD guideline for testing of chemicals, 432, *In vitro* 3T3 NRU phototoxicity test.
Ohyashiki, T., Nunomura, M., Katoh, T., 1999. Detection of superoxide anion radical in phospholipid liposomal membrane by fluorescence quenching method using 1,3-diphenylisobenzofuran. Biochim. Biophys. Acta 1421, 131–139.
Onoue, S., Tsuda, Y., 2006. Analytical studies on the prediction of photosensitive/phototoxic potential of pharmaceutical substances. Pharm. Res. 23, 156–164.

Onoue, S., Igarashi, N., Yamada, S., Tsuda, Y., 2008a. High-throughput reactive oxygen species (ROS) assay: an enabling technology for screening the phototoxic potential of pharmaceutical substances. J. Pharm. Biomed. Anal. 46, 187–193.
Onoue, S., Kawamura, K., Igarashi, N., Zhou, Y., Fujikawa, M., Yamada, H., Tsuda, Y., Seto, Y., Yamada, S., 2008b. Reactive oxygen species assay-based risk assessment of drug-induced phototoxicity: classification criteria and application to drug candidates. J. Pharm. Biomed. Anal. 47, 967–972.
Onoue, S., Yamauchi, Y., Kojima, T., Igarashi, N., Tsuda, Y., 2008c. Analytical studies on photochemical behavior of phototoxic substances; effect of detergent additives on singlet oxygen generation. Pharm. Res. 25, 861–868.
Onoue, S., Seto, Y., Gandy, G., Yamada, S., 2009. Drug-induced phototoxicity; an early *in vitro* identification of phototoxic potential of new drug entities in drug discovery and development. Curr. Drug Saf. 4, 123–136.
Onoue, S., Hosoi, K., Wakuri, S., Iwase, Y., Yamamoto, T., Matsuoka, N., Nakamura, K., Toda, T., Takagi, H., Osaki, N., Matsumoto, Y., Kawakami, S., Seto, Y., Kato, M., Yamada, S., Ohno, Y., Kojima, H., 2013. Establishment and intra-/inter-laboratory validation of a standard protocol of reactive oxygen species assay for chemical photosafety evaluation. J. Appl. Toxicol. 33, 1241–1250.
Onoue, S., Hosoi, K., Toda, T., Takagi, H., Osaki, N., Matsumoto, Y., Kawakami, S., Wakuri, S., Iwase, Y., Yamamoto, T., Nakamura, K., Ohno, Y., Kojima, H., 2014a. Intra-/inter-laboratory validation study on reactive oxygen species assay for chemical photosafety evaluation using two different solar simulators. Toxicol. in Vitro 28, 515–523.
Onoue, S., Kato, M., Yamada, S., 2014b. Development of an albuminous reactive oxygen species assay for photosafety evaluation under experimental biomimetic conditions. J. Appl. Toxicol. 34, 158–165.
Peters, B., Holzhutter, H.G., 2002. In vitro phototoxicity testing: development and validation of a new concentration response analysis software and biostatistical analyses related to the use of various prediction models. Altern. Lab. Anim 30, 415–432.
Quiec, D., Maziere, C., Auclair, M., Santus, R., Gardette, J., Redziniak, G., Franchi, J., Dubertret, L., Maziere, J.C., 1995. Lovastatin enhances the photocytotoxicity of UVA radiation towards cultured N.C.T.C. 2544 human keratinocytes: prevention by cholesterol supplementation and by a cathepsin inhibitor. Biochem. J. 310 (Pt 1), 305–309.
Seto, Y., Kato, M., Yamada, S., Onoue, S., 2013. Development of micellar reactive oxygen species assay for photosafety evaluation of poorly water-soluble chemicals. Toxicol. in Vitro 27, 1838–1846.
Spielmann, H., Liebsch, M., Doring, B., Moldenhauer, F., 1994. First results of an EC/COLIPA validation project of *in vitro* phototoxicity testing methods. ALTEX 11, 22–31.
Spielmann, H., Liebsch, M., Pape, W.J., Balls, M., Dupuis, J., Klecak, G., Lovell, W.W., Maurer, T., De Silva, O., Steiling, W., 1995. EEC/COLIPA in vitro photoirritancy program: results of the first stage of validation. Curr. Probl. Dermatol. 23, 256–264.
Spielmann, H., Balls, M., Dupuis, J., Pape, W.J., Pechovitch, G., de Silva, O., Holzhutter, H.G., Clothier, R., Desolle, P., Gerberick, F., Liebsch, M., Lovell, W.W., Maurer, T., Pfannenbecker, U., Potthast, J.M., Csato, M., Sladowski, D., Steiling, W., Brantom, P., 1998. The international EU/COLIPA in vitro phototoxicity validation study: results of phase II (blind trial). part 1: the 3T3 NRU phototoxicity test. Toxicol. in Vitro 12, 305–327.
Wozniak, M., Tanfani, F., Bertoli, E., Zolese, G., Antosiewicz, J., 1991. A new fluorescence method to detect singlet oxygen inside phospholipid model membranes. Biochim. Biophys. Acta 1082, 94–100.
Xiao, L., Gu, L., Howell, S.B., Sailor, M.J., 2011. Porous silicon nanoparticle photosensitizers for singlet oxygen and their phototoxicity against cancer cells. ACS Nano 5, 3651–3659.
Zhang, J.H., Chung, T.D., Oldenburg, K.R., 1999. A simple statistical parameter for use in evaluation and validation of high throughput screening assays. J. Biomol. Screen. 4, 67–73.

Matsuda *et al. Genes and Environment* (2015) 37:15
DOI 10.1186/s41021-015-0017-5

Genes and Environment

RESEARCH ARTICLE Open Access

# Mutation assay using single-molecule real-time (SMRT™) sequencing technology

Tomonari Matsuda[1,3*], Shun Matsuda[1] and Masami Yamada[2]

## Abstract

**Introduction:** We present here a simple, phenotype-independent mutation assay using a PacBio RSII DNA sequencer employing single-molecule real-time (SMRT) sequencing technology. *Salmonella typhimurium* YG7108 was treated with the alkylating agent *N*-ethyl-*N*-nitrosourea (ENU) and grown though several generations to fix the induced mutations, the DNA was extracted and the mutations were analyzed by using the SMRT DNA sequencer.

**Results:** The ENU-induced base-substitution frequency was 15.4 per Megabase pair, which is highly consistent with our previous results based on colony isolation and next-generation sequencing. The induced mutation spectrum (95% G:C → A:T, 5% A:T → G:C) is also consistent with the known ENU signature. The base-substitution frequency of the control was calculated to be less than 0.12 per Megabase pair. A current limitation of the approach is the high frequency of artifactual insertion and deletion mutations it detects.

**Conclusions:** Ultra-low frequency base-substitution mutations can be detected directly by using the SMRT DNA sequencer, and this technology provides a phenotype-independent mutation assay.

**Keywords:** PacBio RSII DNA sequencer, Single-molecule real-time (SMRT) sequencing technology, Mutation assay

## Introduction

Mutation assays capable of detecting somatic mutations at very low frequencies are important in the areas of environmental mutagenesis, carcinogenesis, epidemiology, and regulatory science. They are especially important in the context of safety evaluation of newly developed drugs or industrial chemicals. Although many mutation assays have been developed, most rely on some kind of phenotypic selection, which involves time-consuming procedures and is potentially biased. We previously reported a phenotype-free mutation assay using next-generation DNA sequencing [1]. In that study, we treated a *Salmonella typhimurium* strain with a mutagen to induced and fix mutations, followed by colony isolation and whole-genome sequencing of the colonies. The induced mutations were successfully detected *in silico* using bioinformatics software. That strategy is summarized in Fig. 1 and named the 'Colony-NGS method'. Although the approach is simple and reliable, difficulties still remain when it is applied to mammalian cells. This is because: 1) the colony-isolation step is much more technically challenging in the case of mammalian cells compared to bacterial cells, and 2) the mammalian genome is diploid and hundreds of times larger than the bacterial genome, which limits deep coverage in sequencing. Furthermore, the Colony-NGS method is not applicable to bio-monitoring of somatic mutations in tissues of experimental animals or clinical specimens from patients because it is impossible to do the colony isolation from those sources.

Recently, 'Duplex Sequencing' methodologies, which enable detecting a single mutation among $>1 \times 10^7$ nucleotides by using a general next-generation DNA sequencing (NGS) technology, have been developed [2,3]. This is a very promising strategy for application to bio-monitoring of somatic mutations. However, here in this paper we demonstrate an alternative approach by using single-molecule real-time sequencing.

The PacBio RS II DNA sequencer (Pacific Biosciences, Inc.) is a recent innovation [4] based on a single-molecule real-time (SMRT) technology. Since it is able to read the sequence of a single DNA molecule, it can in principle detect the mutations present in the molecule

* Correspondence: matsuda.tomonari.8z@kyoto-u.ac.jp
[1]Research Center for Environmental Quality Management, Kyoto University, Shiga, Japan
[3]Tomonari Matsuda, Research Center for Environmental Quality Management, Kyoto University, 1-2 Yumihama, Otsu, Shiga 520-0811, Japan
Full list of author information is available at the end of the article

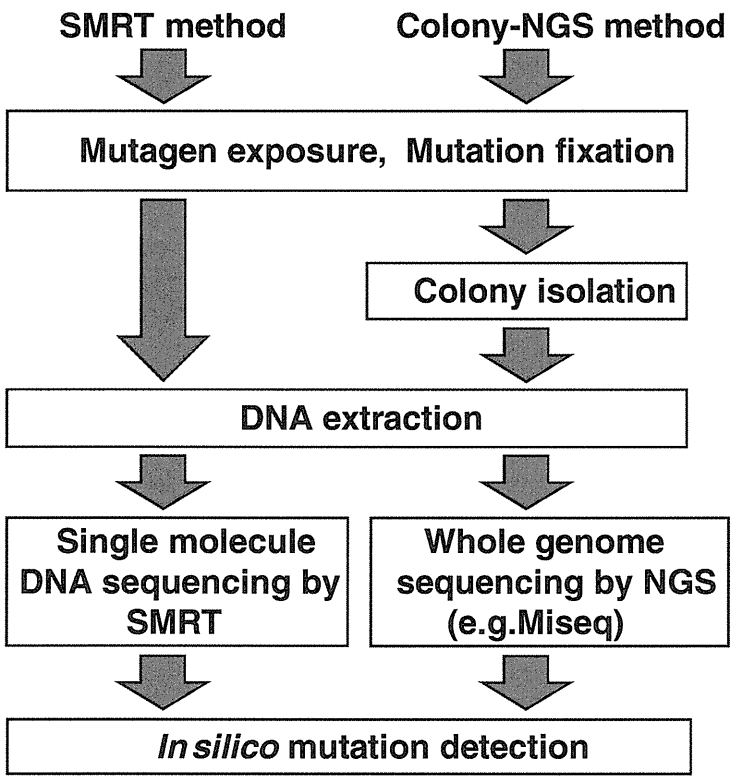


**Fig. 1** Two distinct strategies to detect low-frequency mutations using high-throughput DNA sequencers

just by sequencing it accurately, as summarized in Fig. 1 (named the 'SMRT method') [5]. A significant advantage of this strategy is that the colony isolation step is unnecessary, so that the approach should be applicable to any cell line and specimen from experimental animals, patients and environmental animals.

However, a drawback of this technology is the accuracy of the sequencing data it generates. At present, the error rate in raw reads of the PacBio sequencer is exceedingly high (~15%). To help overcome this problem, the 'SMRTbell™ template', in which single-stranded DNA loops are ligated to both ends of a double-stranded DNA, is used to direct sequencing of the same DNA molecule repeatedly [6]. The greater the number of repeat reads so as to generate a consensus read of multiple sub-reads from the same single circular DNA template – i.e., a circular consensus sequence (CCS) read – the more accurate the sequencing result [7]. In this study, we validated that we can detect ultra-low frequency mutations by using the SMRT method with the CCS strategy.

## Materials and methods

### Materials

ENU (CAS No. 759-73-9) and dimethyl sulfoxide (DMSO; CAS NO. 67-68-5) were purchased from Wako (Osaka, Japan). The test strain *Salmonella typhimurium* YG7108, *hisG46 rfa ΔuvrB bio* $ada_{ST}$::$kan^r$ $ogt_{ST}$::$cat^r$, which is highly sensitive to alkylating agents, was used in this study [8].

### Mutagen exposure and mutation fixation

The exposure method followed the Ames test 20-min pre-incubation procedure [9]. The YG7108 strain was cultured overnight at 37 °C in nutrient broth (No.2, OXOID) containing 25 μg/mL kanamycin and 10 μg/mL chloramphenicol. Phosphate buffer (0.5 mL), DMSO or 2.5 mg/mL ENU (0.1 mL) and the overnight culture (0.1 mL) were mixed in a tube in that order and incubated for 20 min at 37 °C with gentle shaking at 100 rpm. A 1-μL portion was added into 10 mL of LB medium and cultured at 37 °C for 13 h to fix mutations, after which DNA was extracted. The rest of the mixture was poured onto a minimum agar plate in 2 mL of 0.6 % soft agar and incubated for two days at 37 °C, following which the revertant colonies were counted.

### Preparation of SMRTbell™ templates and sequencing

The genomic DNA samples (5 μg each) were sheared to 50-1000 bp (average 280 bp) fragments by using a Covaris Shearing Device, and used to construct a PacBio

DNA library using a SMRTbell Template Prep Kit 1.0 following the manufacturer's guidelines (http://www.pacb.com/samplenet/PC_250bp_Amplicon_Library_Preparation_and_Sequencing.pdf). Each sample was sequenced on the PacBio RS platform on a single SMRT Cell with C2-P4 chemistry. The base calling and CCS read generation was carried out using PacBio's instrument control and SMRT Analysis software.

### *In silico* mutation detection

Mutation detection was carried out by using CLC Genomics Workbench software (ver 7). The fastq files of raw data and CCS were imported into the software. The CCS fastq files were mapped to reference *Salmonella* genome sequences: NC_003197 (*S. typhimurium* str. LT2 chromosome, complete genome, 4,857,432 bp), and CP003387 (*S. typhimurium* str. 798 plasmid p798_93, complete sequence, 93,877 bp). The point mutations were detected using the Basic Variant Detection command (first screening). The essential parameters of the Basic Variant Detection were: ploidy = 1, minimum coverage = 1, minimum count = 1, minimum frequency (%) = 0.1, neighborhood radius = 5, minimum central quality = 40, minimum neighborhood quality = 40. The mutated reads were searched in the CCS fastq files and their corresponding raw reads were extracted from the raw-fastq files. The extracted raw reads were combined in a new fastq file and mapped to the *Salmonella* reference sequence again. The raw reads were manually checked and mutation calls were counted with the help of the viewer function of the CLC Genomics Workbench software.

## Results

The test strain *Salmonella typhimurium* YG7108, which is highly sensitive to alkylating agents, was treated with ENU (Fig. 2a) or its solvent DMSO, followed by dilution and growth overnight in LB medium to fix mutations. Genomic DNA was extracted from the overnight culture. SMRTbell templates were prepared from the DNA samples, with an average insertion size of 280 bp. Note that no PCR amplification step was carried out during preparation of the SMRTbell templates, which is essential to minimize the occurrence of artifactual mutations. The templates were subjected to the sequencing reaction

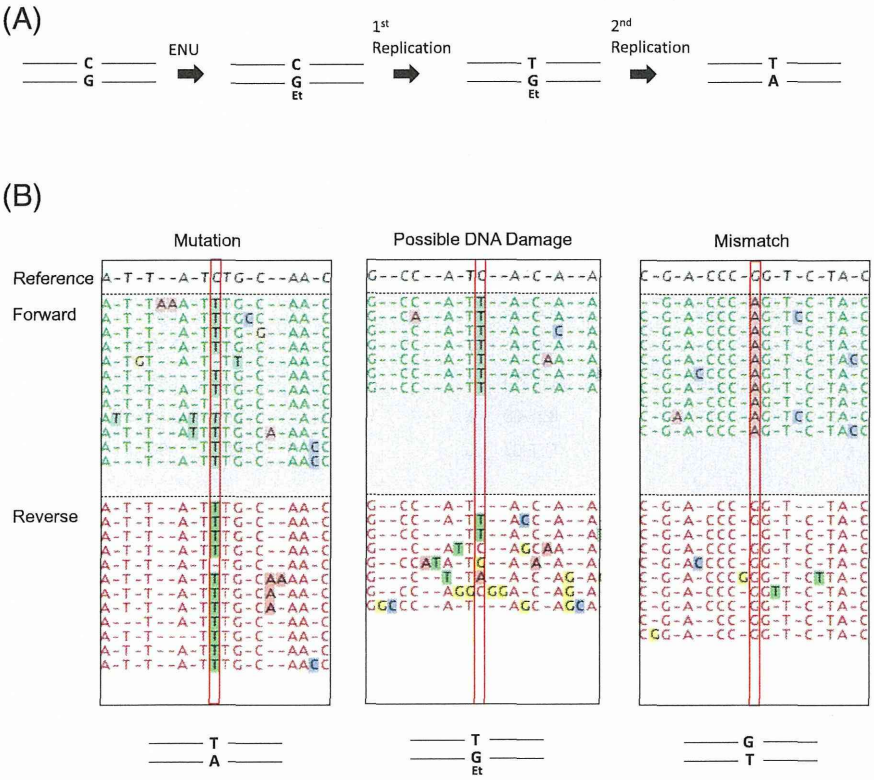


**Fig. 2** Detection of mutations, DNA damage and mismatches by mapping of raw reads of the SMRT sequencer. **a** Example of ENU induction of an alkylated base ($O^6$-ethyl-guanine) in genomic DNA, which will induce a G to A mutation after the 2nd round of replication. **b** Examples of mapped reads. In cases of a real mutation, the same base is clearly called in both the forward and reverse reads. In cases of DNA damage, one strand is mapped clearly but the other strand is not. In cases of mismatch, both the forward and reverse reads are mapped clearly but different bases are called between the forward and reverse reads

**Table 1** Number of mutation-calls at the first screening

| Sample | No. of bases analyzed (Mb) | No. of mutations called | | |
|---|---|---|---|---|
| | | Insertions | Deletions | Base substitutions |
| Control | 8.09 | 405 | 424 | 19 |
| ENU | 8.56 | 376 | 1276 | 160 |

in the PacBio RS II platform, and fastq files were generated from the raw data (contains all the sequence information of multiple sub-reads) and CCS data (contains only the consensus sequence). The threshold of the CCS was a pass time (the number of times the same molecule was repeatedly read) of 10 and 99% accuracy.

The CCS-fastq files were imported to CLC Genomics Workbench software (ver.7). In total, 8.09 and 8.56 Mbp of the sequence data were obtained from the control and ENU-treated samples, respectively. The CCS reads were mapped to the reference sequence of *Salmonella typhimurium* and the point mutations were detected *in silico*. Improbably large numbers of insertions and deletions were called in both the control (405 insertions and 424 deletions) and ENU-treated (367 insertions and 1276 deletions) samples, respectively (Table 1). We had previously analyzed mutations induced in the same bacterial strain with the same exposure protocol by isolating colonies and carrying out whole-genome sequencing. In that previous study, we analyzed the entire genome of each of 4 clones (4.8 Mbp of *Salmonella* genome × 4 clones = 19.6 Mbp search region), but did not detect any insertions and deletions in either the control or ENU-treated samples (unpublished observations). Thus we concluded that the insertions and deletions called in this present study are not reliable and most probably artifacts. In the case of base substitutions, however, 19 and 160 mutations were called in the control and ENU-treated samples, respectively (Table 1). While these frequencies are consistent with the results of our previous study, they are still higher than the estimated values. Thus we decided to proceed with a confirmation step regarding the base substitutions.

Next, we obtained sequence IDs of the CCS reads in which the base substitutions were called at the first screening. Then we searched the sequence IDs in the raw fastq files and extracted the corresponding information of the sequence IDs, and made new fastq files which contained the raw repeated sequence data of the molecules in which the base substitution was possibly present. The newly edited fastq files were mapped to the same *Salmonella* reference sequence. Typical examples of mapped raw reads are shown in Fig. 2b. In the sequencing reaction using the SMRTbell template, the plus

**Table 2** Details of the 19 base substitutions called at the first screening in the control sample

| Reference position | Reference | Forward read | | | | Reverse read | | | | Comment | Judgement | *p*-value** |
|---|---|---|---|---|---|---|---|---|---|---|---|---|
| | | Most dominant allele | Coverage | Read count | *p*-value* | Most dominant allele | Coverage | Read count | *p*-value* | | | |
| 999271 | C | C | 33 | 23 | 3.9E-20 | T | 36 | 30 | 5.5E-31 | | Mismatch | 0 |
| 4778252 | T | T | 17 | 16 | 9.1E-19 | A | 19 | 19 | 4.4E-23 | | Mismatch | 0 |
| 3355477 | 0047 | C | 13 | 12 | 4.4E-14 | G | 11 | 10 | 1.0E-11 | | Mismatch | 1.0E-11 |
| 536849 | C | C | 9 | 9 | 2.5E-11 | T | 9 | 9 | 2.5E-11 | | Mismatch | 5.0E-11 |
| 1051080 | G | A | 10 | 9 | 1.6E-10 | G | 10 | 9 | 1.6E-10 | | Mismatch | 3.1E-10 |
| 3287776 | A | T | 11 | 8 | 8.2E-08 | A | 12 | 11 | 6.7E-13 | | Mismatch | 8.2E-08 |
| 3823422 | C | C | 7 | 4 | 5.7E-03 | G | 11 | 10 | 1.0E-11 | | Mismatch | 5.7E-03 |
| 316363 | G | | | | | | | | | edge of map | No | |
| 694963 | C | | | | | | | | | edge of map | No | |
| 918766 | G | | | | | | | | | edge of map | No | |
| 1922859 | C | | | | | | | | | edge of map | No | |
| 4423790 | C | | | | | | | | | edge of map | No | |
| 4144134 | C | | | | | | | | | No mutation | No | |
| 4515279 | C | | | | | | | | | No mutation | No | |
| 290717 | C | | | | | | | | | original allele | No | |
| 1760048 | A | | | | | | | | | original allele | No | |
| 1760052 | A | | | | | | | | | original allele | No | |
| 3741045 | T | | | | | | | | | original allele | No | |
| 4099877 | G | | | | | | | | | original allele | No | |

*Probability that the real allele is not the most dominant allele
**Probability that the Judgement is not correct

**Table 3** Details of the 160 base substitutions called at the first screening in the ENU-treated sample

| Reference position | Reference position | Forward read | | | | Reverse read | | | | Comment | Judgement | *p*-value** |
|---|---|---|---|---|---|---|---|---|---|---|---|---|
| | | Most dominant allele | Coverage | Read count | *p*-value* | Most dominant allele | Coverage | Read count | *p*-value* | | | |
| 146824 | G | A | 22 | 19 | 1.2E-20 | A | 22 | 18 | 9.9E-19 | | Mutation | 0 |
| 994061 | G | A | 20 | 19 | 2.9E-22 | A | 20 | 17 | 2.4E-18 | | Mutation | 0 |
| 2007634 | G | A | 33 | 24 | 5.9E-22 | A | 31 | 25 | 2.9E-25 | | Mutation | 0 |
| 2044677 | C | T | 24 | 19 | 3.9E-19 | T | 21 | 18 | 1.7E-19 | | Mutation | 0 |
| 2724713 | C | T | 32 | 21 | 3.4E-17 | T | 33 | 22 | 2.5E-18 | | Mutation | 0 |
| 2747120 | G | A | 34 | 24 | 2.9E-21 | A | 37 | 31 | 4.0E-32 | | Mutation | 0 |
| 2871399 | G | A | 32 | 26 | 2.1E-26 | A | 34 | 28 | 1.1E-28 | | Mutation | 0 |
| 2930794 | G | A | 26 | 23 | 2.8E-25 | A | 24 | 18 | 3.0E-17 | | Mutation | 0 |
| 3007696 | A | G | 45 | 33 | 4.8E-30 | G | 47 | 36 | 4.0E-34 | | Mutation | 0 |
| 3322100 | C | T | 21 | 18 | 1.7E-19 | T | 22 | 19 | 1.2E-20 | | Mutation | 0 |
| 3666060 | G | A | 29 | 23 | 5.7E-23 | A | 30 | 22 | 2.2E-20 | | Mutation | 0 |
| 3695370 | G | A | 20 | 17 | 2.4E-18 | A | 21 | 18 | 1.7E-19 | | Mutation | 0 |
| 3708252 | A | G | 29 | 26 | 9.5E-29 | G | 31 | 25 | 2.9E-25 | | Mutation | 0 |
| 3863986 | G | A | 18 | 16 | 5.8E-18 | A | 19 | 16 | 3.5E-17 | | Mutation | 0 |
| 3961843 | G | A | 25 | 20 | 2.8E-20 | A | 25 | 23 | 4.3E-26 | | Mutation | 0 |
| 4320817 | C | T | 21 | 18 | 1.7E-19 | T | 21 | 18 | 1.7E-19 | | Mutation | 0 |
| 2171812 | G | A | 16 | 15 | 1.3E-17 | A | 17 | 15 | 8.4E-17 | | Mutation | 1.1E-16 |
| 327560 | C | T | 23 | 17 | 4.3E-16 | T | 24 | 20 | 4.9E-21 | | Mutation | 4.4E-16 |
| 2209612 | A | G | 16 | 14 | 1.2E-15 | G | 15 | 14 | 2.0E-16 | | Mutation | 1.4E-15 |
| 2705366 | G | A | 24 | 17 | 2.2E-15 | A | 24 | 22 | 6.3E-25 | | Mutation | 2.2E-15 |
| 2215678 | C | T | 30 | 19 | 6.1E-15 | T | 30 | 26 | 6.0E-28 | | Mutation | 6.1E-15 |
| 3881583 | C | T | 15 | 13 | 1.8E-14 | T | 14 | 14 | 3.1E-17 | | Mutation | 1.8E-14 |
| 1368298 | G | A | 16 | 13 | 1.1E-13 | A | 17 | 17 | 9.5E-21 | | Mutation | 1.1E-13 |
| 4840145 | G | A | 16 | 13 | 1.1E-13 | A | 18 | 14 | 4.2E-14 | | Mutation | 1.5E-13 |
| 390064 | C | T | 17 | 13 | 6.1E-13 | T | 19 | 16 | 3.5E-17 | | Mutation | 6.1E-13 |
| 733247 | C | T | 17 | 13 | 6.1E-13 | T | 18 | 16 | 5.8E-18 | | Mutation | 6.1E-13 |
| 3257503 | G | A | 17 | 13 | 6.1E-13 | A | 17 | 16 | 9.1E-19 | | Mutation | 6.1E-13 |
| 935658 | G | A | 18 | 15 | 5.0E-16 | A | 17 | 13 | 6.1E-13 | | Mutation | 6.1E-13 |
| 2316694 | C | T | 17 | 14 | 7.4E-15 | T | 17 | 13 | 6.1E-13 | | Mutation | 6.2E-13 |
| 414142 | G | A | 12 | 11 | 6.7E-13 | A | 12 | 12 | 6.9E-15 | | Mutation | 6.7E-13 |
| 556175 | G | A | 13 | 12 | 4.4E-14 | A | 12 | 11 | 6.7E-13 | | Mutation | 7.1E-13 |
| 355651 | C | T | 38 | 30 | 1.8E-29 | T | 36 | 20 | 7.3E-13 | | Mutation | 7.3E-13 |
| 748721 | C | T | 14 | 12 | 2.7E-13 | T | 12 | 11 | 6.7E-13 | | Mutation | 9.4E-13 |
| 2715604 | C | T | 20 | 14 | 1.2E-12 | T | 24 | 20 | 4.9E-21 | | Mutation | 1.2E-12 |
| 2504585 | C | T | 10 | 10 | 1.6E-12 | T | 10 | 10 | 1.6E-12 | | Mutation | 3.2E-12 |
| 688445 | G | A | 12 | 11 | 6.7E-13 | A | 11 | 10 | 1.0E-11 | | Mutation | 1.1E-11 |
| 222807 | C | T | 18 | 16 | 5.8E-18 | T | 19 | 13 | 1.7E-11 | | Mutation | 1.7E-11 |
| 4652102 | G | A | 19 | 13 | 1.7E-11 | A | 22 | 20 | 1.3E-22 | | Mutation | 1.7E-11 |
| 3117258 | G | A | 25 | 19 | 2.2E-18 | A | 22 | 14 | 3.0E-11 | | Mutation | 3.0E-11 |
| 1005055 | C | T | 16 | 12 | 8.9E-12 | T | 14 | 11 | 2.4E-11 | | Mutation | 3.2E-11 |
| 2264426 | G | A | 11 | 10 | 1.0E-11 | A | 9 | 9 | 2.5E-11 | | Mutation | 3.5E-11 |
| 992465 | C | T | 14 | 11 | 2.4E-11 | T | 14 | 11 | 2.4E-11 | | Mutation | 4.7E-11 |
| 1076365 | G | T | 12 | 10 | 6.1E-11 | T | 12 | 11 | 6.7E-13 | | Mutation | 6.2E-11 |

**Table 3** Details of the 160 base substitutions called at the first screening in the ENU-treated sample *(Continued)*

| | | | | | | | | | | | |
|---|---|---|---|---|---|---|---|---|---|---|---|
| 458994 | C | A | 29 | 26 | 9.5E-29 | A | 23 | 14 | 1.4E-10 | Mutation | 1.4E-10 |
| 3062433 | C | T | 18 | 14 | 4.2E-14 | T | 13 | 10 | 3.5E-10 | Mutation | 3.5E-10 |
| 421079 | G | T | 8 | 8 | 4.0E-10 | T | 9 | 9 | 2.5E-11 | Mutation | 4.2E-10 |
| 4736812 | C | A | 24 | 14 | 6.4E-10 | A | 18 | 16 | 5.8E-18 | Mutation | 6.4E-10 |
| 2957288 | C | T | 12 | 12 | 6.9E-15 | T | 11 | 9 | 9.4E-10 | Mutation | 9.4E-10 |
| 3872165 | C | T | 11 | 9 | 9.4E-10 | T | 10 | 10 | 1.6E-12 | Mutation | 9.4E-10 |
| 278409 | G | T | 19 | 12 | 1.2E-09 | T | 23 | 14 | 1.4E-10 | Mutation | 1.4E-09 |
| 2861538 | G | A | 15 | 13 | 1.8E-14 | A | 14 | 10 | 1.9E-09 | Mutation | 1.9E-09 |
| 1408682 | G | A | 9 | 8 | 2.4E-09 | A | 9 | 9 | 2.5E-11 | Mutation | 2.5E-09l |
| 272653 | C | A | 10 | 9 | 1.6E-10 | A | 9 | 8 | 2.4E-09 | Mutation | 2.6E-09 |
| 2757635 | G | T | 9 | 8 | 2.4E-09 | T | 8 | 8 | 4.0E-10 | Mutation | 2.8E-09 |
| 4148066 | C | A | 9 | 8 | 2.4E-09 | A | 8 | 8 | 4.0E-10 | Mutation | 2.8E-09 |
| 206275 | | T | 17 | 11 | 3.6E-09 | T | 14 | 11 | 2.4E-11 | Mutation | 3.6E-09 |
| 250264 | C | T | 9 | 8 | 2.4E-09 | T | 9 | 8 | 2.4E-09 | Mutation | 4.9E-09 |
| 2425294 | C | T | 9 | 8 | 2.4E-09 | T | 9 | 8 | 2.4E-09 | Mutation | 4.9E-09 |
| 4431921 | G | A | 12 | 9 | 5.4E-09 | A | 12 | 10 | 6.1E-11 | Mutation | 5.4E-09 |
| 909863 | C | T | 31 | 16 | 5.5E-09 | T | 31 | 17 | 9.6E-11 | Mutation | 5.6E-09 |
| 1085221 | G | A | 12 | 9 | 5.4E-09 | A | 12 | 9 | 5.4E-09 | Mutation | 1.1E-08 |
| 2250730 | G | A | 10 | 10 | 1.6E-12 | A | 10 | 8 | 1.5E-08 | Mutation | 1.5E-08 |
| 662822 | G | A | 21 | 12 | 2.8E-08 | A | 19 | 18 | 4.3E-21 | Mutation | 2.8E-08 |
| 731542 | C | T | 13 | 9 | 2.9E-08 | T | 13 | 11 | 4.1E-12 | Mutation | 2.9E-08 |
| 412934 | G | A | 8 | 7 | 3.9E-08 | A | 10 | 8 | 1.5E-08 | Mutation | 5.3E-08 |
| 2104411 | C | T | 11 | 8 | 8.2E-08 | T | 12 | 10 | 6.1E-11 | Mutation | 8.2E-08 |
| 4189314 | G | A | 15 | 13 | 1.8E-14 | A | 14 | 9 | 1.5E-07 | Mutation | 1.5E-07 |
| 3364045 | C | T | 14 | 9 | 1.5E-07 | T | 15 | 12 | 1.6E-12 | Mutation | 1.5E-07 |
| 2795479 | C | T | 6 | 6 | 1.0E-07 | T | 6 | 6 | 1.0E-07 | Mutation | 2.1E-07 |
| 555449 | G | A | 9 | 7 | 2.3E-07 | A | 9 | 9 | 2.5E-11 | Mutation | 2.3E-07 |
| 1306236 | G | A | 12 | 8 | 4.5E-07 | A | 12 | 10 | 6.1E-11 | Mutation | 4.5E-07 |
| 4173104 | G | A | 9 | 7 | 2.3E-07 | A | 9 | 7 | 2.3E-07 | Mutation | 4.6E-07 |
| 2260312 | C | T | 8 | 7 | 3.9E-08 | T | 7 | 6 | 6.3E-07 | Mutation | 6.7E-07 |
| 2873628 | G | A | 6 | 6 | 1.0E-07 | A | 7 | 6 | 6.3E-07 | Mutation | 7.4E-07 |
| 1219556 | C | T | 9 | 7 | 2.3E-07 | T | 7 | 6 | 6.3E-07 | Mutation | 8.6E-07 |
| 3929806 | C | T | 17 | 13 | 6.1E-13 | T | 18 | 10 | 1.2E-06 | Mutation | 1.2E-06 |
| 719703 | G | A | 10 | 7 | 1.3E-06 | A | 9 | 8 | 2.4E-09 | Mutation | 1.3E-06 |
| 767167 | C | T | 10 | 7 | 1.3E-06 | T | 11 | 8 | 8.2E-08 | Mutation | 1.4E-06 |
| 4671425 | C | T | 5 | 5 | 1.7E-06 | T | 7 | 7 | 6.3E-09 | Mutation | 1.7E-06 |
| 74626 | G | A | 5 | 5 | 1.7E-06 | A | 6 | 6 | 1.0E-07 | Mutation | 1.8E-06 |
| 1556611 | G | A | 5 | 5 | 1.7E-06 | A | 6 | 6 | 1.0E-07 | Mutation | 1.8E-06 |
| 3771665 | G | A | 13 | 8 | 2.3E-06 | A | 13 | 10 | 3.5E-10 | Mutation | 2.3E-06 |
| 1277370 | C | T | 10 | 7 | 1.3E-06 | T | 10 | 7 | 1.3E-06 | Mutation | 2.6E-06 |
| 2831234 | G | A | 8 | 6 | 3.7E-06 | A | 8 | 8 | 4.0E-10 | Mutation | 3.7E-06 |
| 4834248 | G | A | 16 | 9 | 3.8E-06 | A | 17 | 15 | 8.4E-17 | Mutation | 3.8E-06 |
| 4640576 | G | A | 12 | 10 | 6.1E-11 | A | 11 | 7 | 6.9E-06 | Mutation | 6.9E-06 |
| 314407 | C | T | 11 | 7 | 6.9E-06 | T | 10 | 9 | 1.6E-10 | Mutation | 6.9E-06 |
| 1799318 | G | A | 9 | 8 | 2.4E-09 | A | 6 | 5 | 1.1E-05 | Mutation | 1.1E-05 |